THE AMERICAN MINERALOGIST
JOURNAL OF THE MINERALOGICAL SOCIETY OF AMERICA

Vol. 24 NOVEMBER, 1939 No. 11

VARIATION OF HARDNESS IN THE DIAMOND[1]

EDWARD H. KRAUS AND CHESTER B. SLAWSON,
University of Michigan, Ann Arbor, Michigan.

INTRODUCTION

It has long been known that hardness is a vector property. For many substances hardness curves have been determined showing that this property varies with the different crystal faces of the substance and also with the direction on the faces. That the hardness of the diamond varies materially in this manner has been common knowledge to diamond cutters. Unfortunately erroneous statements concerning the variation of the hardness of the diamond have found their way into mineralogical literature, and only in recent years have efforts been made to correct these statements. Significant contributions to our knowledge of the hardness of the diamond and its relation to crystal structure and to cutting for gem and industrial purposes have been made by W. Fr. Eppler, H. Rose, K. Schlossmacher, and more recently by H. Bergheimer. It is the purpose of this paper to discuss the variation of the hardness in the diamond, as established by the experience of diamond cutters, in terms of crystallographic theory, crystal structure, valence bonds, cleavage, and growth and solution phenomena.

VARIATION OF HARDNESS WITH THE CRYSTAL FACE

In the sixth edition of Dana's *System of Mineralogy*,[2] published in 1892, the hardness of the diamond is given, as is customary, as 10. However, there is also the statement that the hardness is greater on the faces of the cube than on those of the octahedron, but without reference to the source or the basis for the statement. Similar statements were subsequently made by M. Bauer,[3] G. Tschermak,[4] F. Zirkel,[5] H. Miers,[6] C. Hintze,[7] A. Sauer,[8] and others.

---

[1] A large part of the material of this article was presented in abstract form, or in considerable detail, illustrated with lantern slides showing many of the figures, at the following meetings:

December 28, 1938, The Mineralogical Society of America, New York City.
March 15, 1939, Research Club of the University of Michigan, Ann Arbor.
March 17, 1939, The Michigan Academy of Science, Arts and Letters, Ann Arbor.
April 24, 1939, Conclave of the American Gem Society, Chicago.

At each of these meetings a discussion followed the reading of the paper.

[2] P. 4.

In 1925 Eppler and Rose[9] called attention to the fact that experience showed that the statements commonly found in mineralogical texts are incorrect and that the octahedron faces of the diamond are materially harder than those of the cube. They also indicated that the faces of the rhombic dodecahedron have an intermediate hardness. In spite of these published observations statements have continued to be made in some texts[10] that the cube faces are the hardest.

Both Eppler[11] and Schlossmacher[12] have discussed at length the variation of the hardness in relation to diamond cutting and confirmed the earlier statements by Eppler and Rose. They also pointed out that diamond cutters have long known that the hardness is greatest on faces of the octahedron, and that it varies materially with direction. The optimum directions for cutting or grinding, commonly designated as polishing, as given by them are those which are parallel to a crystallographic axis. Similar statements have been made by Bergheimer.[13] Accordingly, the following generalizations may be made:

(1) Since faces of the cube *h* (Fig. 1) are parallel to two crystallographic axes, there are two optimum polishing directions on each of these faces. Facets parallel to these faces are the easiest to polish.

(2) Faces of the rhombic dodecahedron *d* are parallel to one cyrstallographic axis. Consequently each face has one optimum direction, which is parallel to the short diagonal of the face.

(3) Since octahedron faces *o* are equally inclined to the three crystallographic axes, these faces show the greatest possible divergence from parallelism with the axes. They are accordingly the most difficult to

---

[3] (*a*) *Lehrbuch der Mineralogie*, Second Edition, 244 (1904).
(*b*) *Edelsteinkunde*, Second Edition, 154 (1909).

[4] *Lehrbuch der Mineralogie*, Sixth Edition, 383 (1905).

[5] Naumann-Zirkel, *Lehrbuch der Mineralogie*, Tenth Edition, 402 (1898).

[6] *Mineralogy*, 294 (1902).

[7] *Handbuch der Mineralogie*, 5 (1904).

[8] *Mineralkunde*, 123 (1905).

[9] Einige Beobachtungen am Diamant, *Centralbl. Mineral., Geol., und Pal.*, 251–253 (1925).

[10] Williams, A. F., *Genesis of the Diamond*, Vol. **II**, 465 (1932).
Klockmann, F., *Lehrbuch der Mineralogie*, revised by P. Ramdohr, Eleventh Edition, 292 (1936).

[11] (*a*) *Der Diamant und seine Bearbeitung* (1933).
(*b*) *Edelsteine und Schmucksteine* (1934).

[12] Bauer's *Edelsteinkunde*, Third Edition (1932).

[13] Die Schleifhärte des Diamanten und seine Struktur: *Neues Jahrb. fuer Mineral., Geol., und Pal.*, **74**, 318–332 (1938).

polish. Indeed, it is impossible to make any progress on such faces or on planes exactly parallel to them.[14]

CRYSTALLOGRAPHIC THEORY

The stereographic projection showing the faces of the cube {001}, rhombic dodecahedron {101}, and octahedron {111} (Fig. 2), may be used to indicate the transition in hardness from one face to another in terms of the above statements, and also to give the optimum directions.

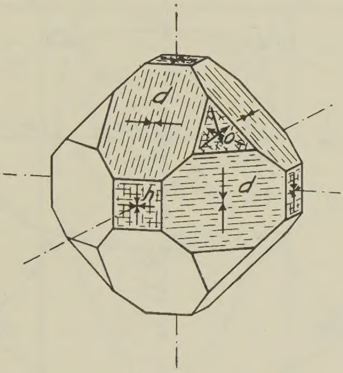

FIG. 1. Diamond crystal showing *grain* and optimum polishing and sawing directions on faces of the cube *h*, rhombic dodecahedron *d*, and octahedron *o*.

The variation in hardness is approximately indicated by the length of the arrows, that is, the longer the arrow the more readily the polishing takes place. Hence, the hardness of the planes with the longest arrows is less in the directions indicated than on other planes or in other directions. In other words, it is evident that the change in hardness from one face or from one direction to another is not abrupt but gradual. This is in accord with the observations on the variation of hardness in other substances, and the behavior of vector properties in general.

The projection also shows that the sense of direction is of much importance, as for example, on octahedron faces where polishing must always be in directions perpendicular to and toward the edges of the face. These are the directions that tend to approximate parallelism to a crystallographic axis. It must be borne in mind, however, that to make progress, even in these favorable directions, the plane must not be exactly parallel to the octahedron face, but be somewhat inclined to it. The dashed lines in the projection indicate directions in which no progress in polishing can be made with diamond dust.

---

[14] Compare E. H. Kraus, and C. B. Slawson, *Gems and Gem Materials*, Third Edition, 98 (1939).

Crystal Structure

The foregoing observations can be shown to be in full accord with the crystal structure of the diamond which has been accurately determined by the Braggs and intensively studied by others. A careful study of a model which gives the spatial arrangement of the carbon atoms in the diamond (Fig. 3) and their distribution in various planes, reveals the following facts:

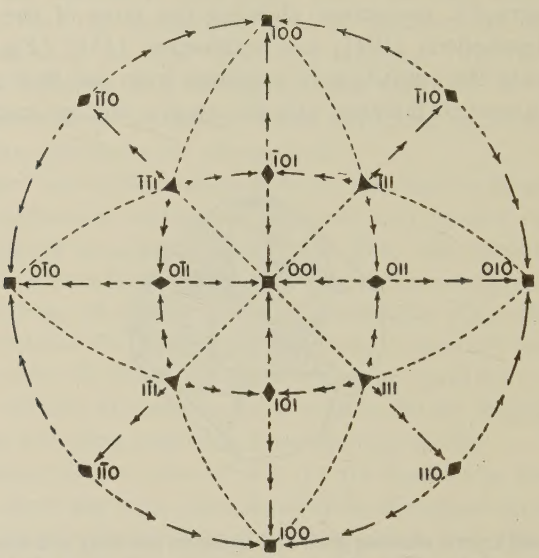

Fig. 2. Stereographic projection of cube, dodecahedron and octahedron, showing variations in hardness.

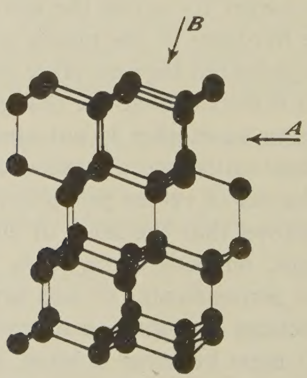

Fig. 3. Model showing the crystal structure of the diamond.

(1) In the direction of the crystallographic axes A the atoms are uniformly and widely separated (Figs. 4 and 5).

(2) As the atoms are uniformly spaced in these directions, hardness is, hence, bivector in character. There is no sense of direction (Fig. 1).

(3) No valence bonds lie in these directions.

(4) The crystallographic axes intersect valence bonds at larger angles than do any other directions through the structure.

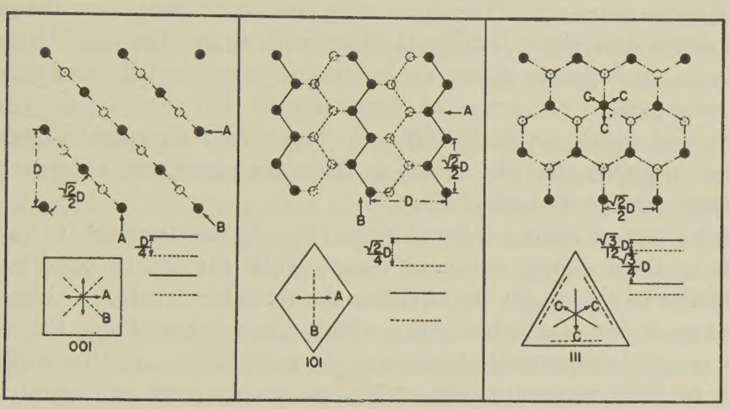

Fig. 4 Fig. 5 Fig. 6

Fig. 4. Diagrams showing (a) distribution of atoms in cube planes, (b) spacing of successive parallel planes, (c) optimum directions for polishing and sawing *A*, and (d) directions of greatest resistance *B*.

Fig. 5. Same for rhombic dodecahedron planes.

Fig. 6. Same for octahedron planes. The three optimum polishing directions are indicated by *C*.

These facts indicate that in the direction of the three crystallographic axes the forces holding the structure together can be most readily overcome. This is in full accord with the experience of diamond cutters, already referred to, namely, that the optimum directions for polishing are parallel to the crystallographic axes *A* (Fig. 4). Moreover, the distribution of the atoms in planes parallel to two crystallographic axes, that is, in the planes of the cube (Fig. 4) is such that the reticular density is less than in rhombic dodecahedral (Fig. 5) or octahedral (Fig. 6) places. Accordingly, the faces of the cube are the easiest to polish. This fact has also been long known to diamond cutters. It is therefore obvious why it is advantageous to cut diamonds so that the table is parallel to a face of the cube. In the diamond cutting industry, diamonds cut in this manner are known as *four-point stones*.

In the diagonal directions B in the cube planes (Fig. 4) the distribution of the atoms is closer than in the direction of the crystallographic axes A. Moreover, it is such that the spacing of them in successive planes is staggered. These directions should hence offer much resistance to polishing, which is in accord with experience. In the stereographic projection (Fig. 2) these directions (B) are dashed to indicate their extreme hardness.

As has already been pointed out, octahedral planes are equally inclined to the three crystallographic axes, and accordingly show the greatest possible divergence from parallelism with them. The distribution of atoms in these planes shows an hexagonal pattern with close spacing. The arrangement of successive planes is such that they are alternately closely and widely separated (Fig. 6). The closely separated planes are so close together that the atoms in them are sometimes considered as forming "puckered" carbon rings.[15]

Each atom of these puckered rings (Fig. 3) has three of its valence bonds in these closely arranged planes while the fourth bond is perpendicular to the planes. In addition the reticular density of the atoms is greater in the octahedral planes than in any other. Thus, the atoms in these closely separated planes are held most firmly together while the bonds between successive pairs of such planes are weak and readily ruptured. In this way the superior hardness of the octahedral planes can be explained as also the fact that, due to the wide separation of successive pairs of planes, cleavage takes place easily parallel to them. Figure 3 shows this structure and the direction of two of the cleavages, A and B.

As shown in Fig. 6 the arrangement of the atoms in these closely arranged pairs of planes is such that the sense of direction is important. The direction of polishing should be perpendicular to the intersection of two adjacent octahedral faces, or in other words in directions that approach the short diagonals of the rhombic dodecahedron. As has already been pointed out, these diagonals are parallel to a crystallographic axis. The opposite direction is unfavorable because it is toward and approaches the diagonal of the cube face, which is very resistive. The favorable direction may also be indicated as the one that bisects two adjacent valence bonds between atoms in successively closely spaced planes, directions C (Fig. 6).

To determine these directions the diamond cutter makes use of the so-called *grain* indicated by the growth lines which are parallel to the intersections of octahedral faces (Fig. 1). It must be again emphasized that even in these more favorable directions no progress in polishing can

[15] Clark, G. L., *Applied X-Rays*, Second Edition, 308 (1932).

be made if the facet is exactly parallel to the octahedral plane. To make progress the facet must be somewhat inclined away from the octahedron plane, and obviously the more it is inclined, the more it will approximate a face of the rhombic dodecahedron. Diamonds which are cut with the table approximately parallel to an octahedral plane are called *three-point stones.*

Faces of the rhombic dodecahedron are parallel to one crystallographic axis and intersect the other two axes at equal angles. Accordingly, one direction, that of the short diagonal of the face, is most favorable for polishing. The direction of the long diagonal shows the greatest possible divergence from parallelism with an axis, and hence offers extreme resistance to polishing.

These observations are also in accord with the arrangement of the atoms in the rhombic dodecahedron plane (Fig. 5). Each atom has two valence bonds in the plane, that is, they are co-planar. In the direction A, that of the short diagonal, the atoms are widely spaced and the valence bonds make large angles with this direction. The A direction is favorable for polishing. The direction of the long diagonal B, in which the atoms are more closely spaced and the co-planar bonds are intersected at small angles, is unfavorable. Diamonds cut with the table parallel to a face of the rhombic dodecahedron are called *two-point stones.*

From the above considerations it is obvious that the rhombic dodecahedral planes are intermediate between those of the cube and octahedron with respect to the facility with which they may be polished, those of the cube being the easiest and those of the octahedron the most difficult.

Valence Bonds

It may well be assumed that the ease or difficulty of cleavage parallel to different planes, the variation in hardness, and the effects of solution upon a crystal are largely determined by the forces or valence bonds which hold the atoms in their structural positions. As the crystal structure of the diamond is well known it is possible to calculate approximately the valence bonds for unit areas and thus determine their relation to cleavage, hardness, and solution effects.

Cleavage

The comparative ease or difficulty with which cleavage can take place parallel to certain planes may be determined by calculating the forces or valence bonds per atom which exist between unit areas of successive parallel layers of atoms. That this can be done for the diamond has already been pointed out by Ewald,[16] Mohr[17] and Bergheimer.[18]

Cube planes are uniformly separated one from another and each atom in these planes has two valence bonds which extend to atoms in the next successive parallel layer. Rhombic dodecahedral planes are also uniformly separated, but each atom has only one such valence bond between successive layers. In the case of octahedron planes the successive layers are not uniformly separated, but are alternately widely and closely arranged. In the case of the widely separated planes there is only one such valence bond, while for those planes that are closer together there are three bonds which must be taken into consideration. Professor Kasimir Fajans has very kindly calculated the relative number of bonds per atom for unit areas (D^2) for successive parallel layers of atoms for the above-mentioned four types of planes. His results are as follows:

	D^2
Octahedron (wide)	$4/3\sqrt{3} = 1$
Rhombic dodecahedron	$2\sqrt{2} = 1.22$
Cube	$4 = 1.73$
Octahedron (close)	$4\sqrt{3} = 3$

It is thus evidence that cleavage should take place readily parallel to the octahedron and also that there is a possible cleavage parallel to the rhombic dodecahedron of which some diamond cutters, especially Mr. Lazare Kaplan, make practical use.

These values obtained by Fajans agree with those given by Mohr. The value 1.22 calculated by Fajans and Mohr for the rhombic dodecahedron differs from that obtained by Ewald, namely, 1.53, but the relative order of the various planes is the same. Mohr has already called attention to this difference in the published values for the rhombic dodecahedron.

Hardness

As indicated by Bergheimer,[19] the values obtained above for cleavage cannot be used to estimate the relative hardness per unit area on the different crystal surfaces. To do this it would seem necessary that the valence bonds per atom which lie in the plane must also be taken into consideration. In the case of the cube and octahedron planes there are no additional bonds to be considered. However, each atom in a dodecahedral plane has two bonds lying in that plane (Fig. 5) which are equivalent to one additional effective bond. When this fact is taken into consideration the following relationship is obtained:

---

[16] *Annalen der Physik*, **44**, 281 (1914).

[17] *Abhandlung, Heidelberger Akademie der Wissenschaft, Math-Nat. Klasse, Abteilung* **A**, 12 Abhd., 34 (1924).

[18] Reference 13, p. 330.

[19] Reference 13, p. 330.

Cube	$4 = 1$
Rhombic dodecahedron	$4\sqrt{2} = 1.414$
Octahedron (close)	$4\sqrt{3} = 1.732$

These values would indicate that experience and theory are well in agreement, namely, that the hardness should be greatest on the octahedron, least on the cube, and intermediate on the rhombic dodecahedron.

Solution effects

When a solution acts upon a crystal, the atoms in the layer attacked are removed individually. The relative ease or difficulty with which the different crystal planes may yield to solution can be approximately determined by calculating the number of atoms per unit area, and of the bonds between the atoms in the plane itself, and of those connecting them with the atoms in the next succeeding layer. This calculation leads to ratios that are identical with those obtained for hardness, namely.

Cube	1
Rhombic dodecahedron	1.414
Octahedron	1.732

Accordingly, from the standpoint of structural relations it appears that solution should take place most easily upon faces of the cube and most slowly upon those of the octahedron, and that the rhombic dodecahedron planes occupy an intermediate position. These conclusions are in full accord with the observations of Fersmann and Goldschmidt.[20]

OPTIMUM DIRECTIONS ON FACETS

In the various public presentations of this paper (Footnote 1) it was shown by lantern slides, that since the various facets may be considered as crystal planes, the stereographic projection (Fig. 7) may be used to indicate their location and also the optimum directions on them for polishing. Figure 8 is a projection of the crown or upper part of a four-pointed brilliant cut diamond, where a cube face (001) is the table. This method has also been used by Bergheimer in a recently published paper.[21]

The basis of Fig. 8 is the projection as given in Fig. 7, which shows the transition in hardness from one face to another. The various facets of the crown are located upon this projection and the optimum directions for polishing are readily determined from the basic projection. The relative ease or difficulty of polishing the various facets can be estimated from the lengths of the arrows on the adjacent zones through the cube,

---

[20] Reference 27, Text, XI.

[21] Bergheimer, H., Die Schleifrichtungen auf den Facetten des Diamantbrillianten; *Neues Jahrb. fuer Mineral., Geol., und Pal.*, **75**, 145–158 (1939).

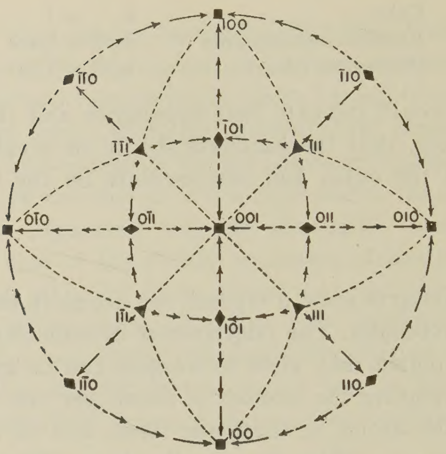

FIG. 7

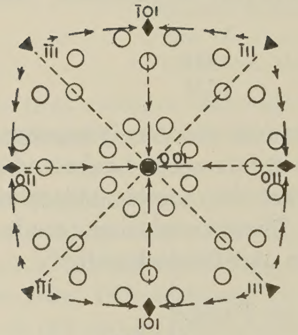

FIG. 8

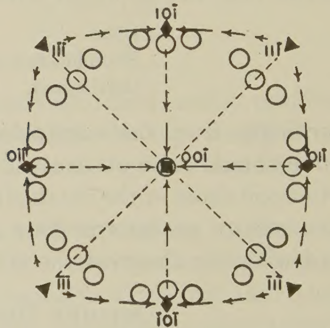

FIG. 9

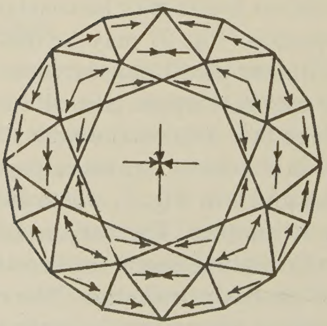

FIG. 10

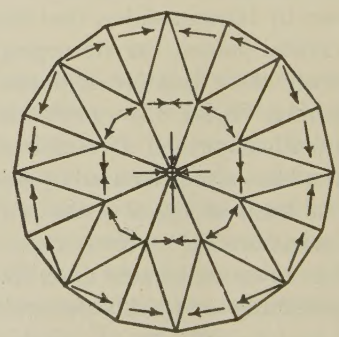

FIG. 11

Figs. 7–11. Projections showing a diamond crystal cut as a four-point brilliant. Fig. 7, stereographic projection showing hardness variation; Figs. 8 and 9, location of crown and pavilion facets, respectively; Figs. 10 and 11, optimum polishing directions of crown and pavilion facets, respectively.

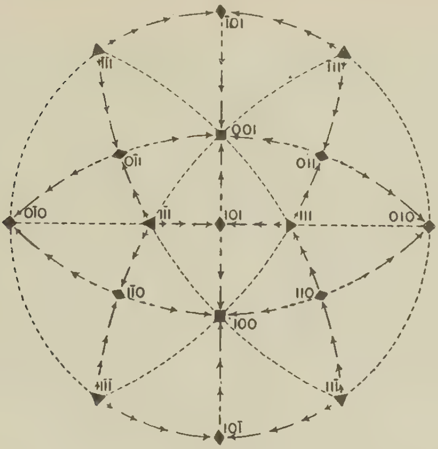

FIG. 12

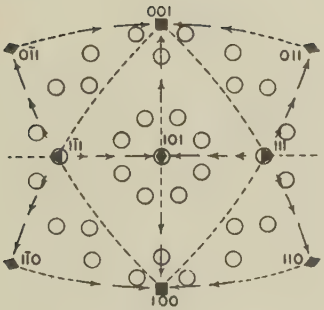

FIG. 13

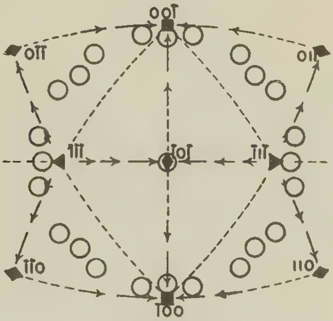

FIG. 14

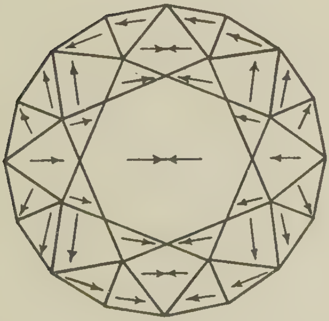

FIG. 15

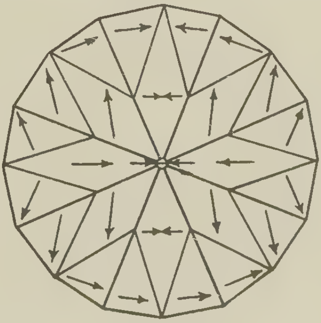

FIG. 16

Figs. 12–16. Projections showing a diamond crystal cut as a two-point brilliant. Fig. 12, stereographic projection showing hardness variation; Figs. 13 and 14, location of crown and pavilion facets, respectively; Figs. 15 and 16, optimum polishing directions of crown and pavilion facets, respectively.

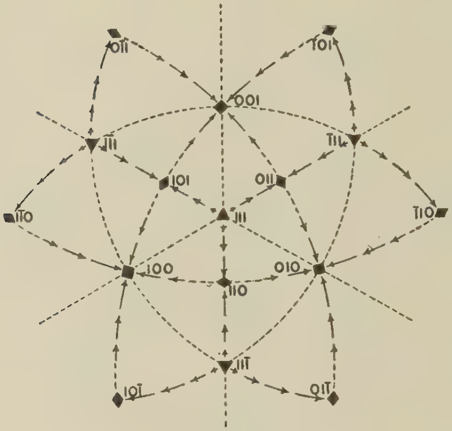

FIG. 17

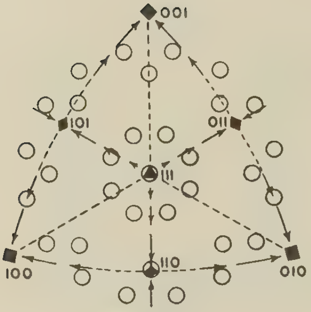

FIG. 18

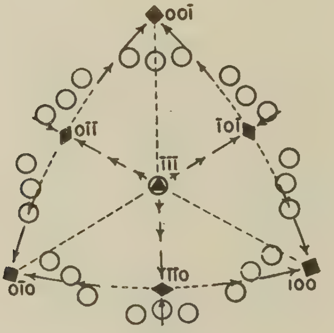

FIG. 19

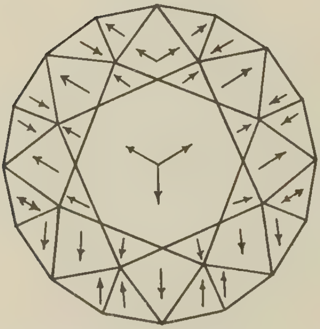

FIG. 20

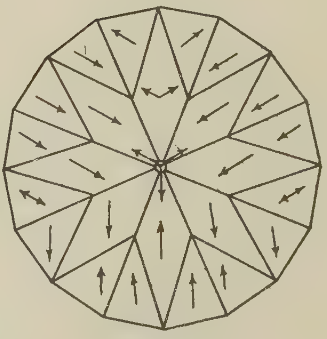

FIG. 21

FIGS. 17–21. Projections showing a diamond crystal cut as a three-point brilliant. Fig. 17, stereographic projection showing hardness variation; Figs. 18 and 19, location of crown and pavilion facets, respectively; Figs. 20 and 21, optimum polishing directions of crown and pavilion facets, respectively.

rhombic dodecahedron, or octahedron. The location of the facets upon the projection will obviously depend upon the fundamental angles used in cutting the diamond. Practice in this regard varies somewhat.[22] The positions given in Fig. 8 and in subsequent figures are based upon the calculations of Tolkowsky,[23] and represent fairly accurately the usual American practice. A comparison of these figures with those of Eppler and Klüppelberg, and Bergheimer will accordingly show some slight differences both as to position and optimum cutting direction.

Figure 9 shows the projection of the pavilion, or back, of a four-point stone. To make these relationships clearer arrows showing optimum polishing directions and ease of cutting may be placed upon a projection of a facetted stone. Figures 10 and 11 give these conditions for the crown and pavilion of a four-point stone. Similar projections have been used by Bauer,[24] Eppler[25] and Bergheimer.[26] Figures 12–16 and 17–21 are corresponding projections for two-point and three-point stones, respectively.

Growth and Solution Phenomena

In 1911 A. von Fersmann and V. Goldschmidt[27] published the results of their exhaustive study of the growth and solution phenomena to be observed on the fundamental crystal faces of the diamond, namely, on the octahedron, rhombic dodecahedron, and cube. These studies were made before the development of x-ray analysis for the determination of crystal structure. Accordingly, it is our purpose to discuss briefly some of their observations and conclusions in terms of crystal structure and valence bonds.

Fersmann and Goldschmidt made the fundamental assumption that the principal or main faces or planes of growth are those in which the attractive forces are the greatest, while the principal faces or planes of solution are those in which the attractive forces are the weakest. Their observations were made on a large number of crystals of diamonds from various localities and led them to postulate that (1) the octahedron is the main growth face, that is, these faces tend to develop more rapidly than the others; (2) the main solution face is that of the cube, that is, these faces are most readily attacked by solvents; and (3) faces of the rhombic dodecahedron occupy a somewhat intermediate position.

---

[22] Reference 14, pp. 83–85.

Also, Eppler, W. Fr., and Klüppelberg, E. Der Praktische Brilliantschliff des Diamanten; *Neues Jahrb. fuer Mineral.* etc., **75**, 135–140 (1939).

[23] Tolkowsky, L., *Diamond Design*, London (1919).

[24] *Edelsteinkunde*, First Edition, 277 (1896).

[25] Reference 11*a*, pp. 126–152.

[26] Reference 21, pp. 152–153.

[27] *Der Diamant*, Text and Atlas (1911).

Figures 22, 23, and 24 taken from the Atlas[28] of Fersmann and Goldschmidt indicate different stages in the growth of octahedral faces. These figures also show the manner of development of the growth lines or *grain*,[29] upon which the diamond cutter places so much reliance for the proper orientation of the crystal.

FIG. 22

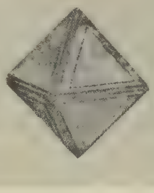

FIG. 23

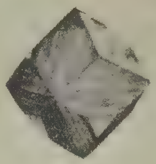

FIG. 24

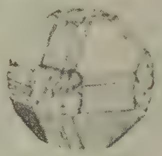

FIG. 25

FIG. 22. Diamond octahedron.

FIGS. 23 and 24. Diamond crystals showing the development of growth lines or *grain*.

FIG. 25. Diamond crystal showing the effect of solution on the faces of the cube.

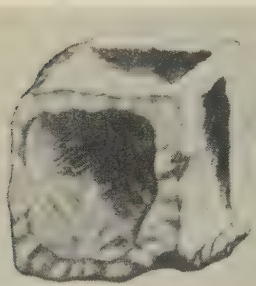

FIG. 26

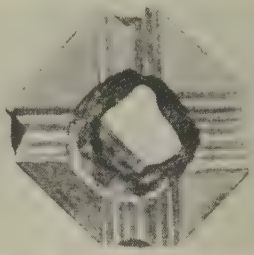

FIG. 27

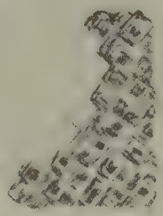

FIG. 28

FIGS. 26 and 27. Diamond crystals showing marked effects of solution on faces of the cube.

FIG. 28. Characteristic solution effects on cube face (greatly enlarged).

According to Fersmann and Goldschmidt, Fig. 25[30] shows the effects of both growth and solution phenomena. The octahedron faces are growth forms, while the action of solution is evident on the faces of the cube. That solution may cause deep depressions, and even holes, on the cube faces is shown by Figs. 26[31] and 27.[32] Moreover, the effect of solution is such that characteristic outlines or figures are often formed on the cube face. These are evident in Figs. 26 and 28.[33] These designs were interpreted by them to be the result of the probable joint action of solution and growth. For it is stated that "the principal solution current attacks the crystal at right angles to the cube face and flows away over the rhombic dodecahedron." Also that "if the mother liquor is strongly solvent, the current will continue to cause solution, but if it is only slightly solvent it may become neutral during its course, and finally lead to deposition and growth. Consequently, it may occur that while solution takes place on the cube face, particles may be deposited on the octahedron."[34]

---

[28] Plate 5, crystals 2, 5, and 4.

[29] See p. 666.

[30] *Atlas*, Plate 17, crystal 50.

[31] *Ibid.*, Plate 23, crystal 69.

[32] *Ibid.*, Plate 17, crystal 49.

Thus, the central portion of each design, Fig. 28, is said to be caused by solution, while the outline or ridges are assumed to be the result of growth. It is also pointed out by them that these ridges are in the zone of the cube and octahedron. In other words, the directions of these ridges indicate intersections of octahedral planes with those of the cube. In view of the earlier discussions under crystal structure and valence bonds it is suggested that there may be another explanation for these interesting outlines on the faces of the cube. These outlines must not be confused with growth lines or *grain*.

Since these ridges may be assumed as the intersections of octahedral and cube planes, it seems quite logical to assume that the ridges are the result of the greater resistance to solution of the closely spaced atoms and the greater strength of the valence bonds in the octahedral planes, rather than that solution and growth take place simultaneously in areas of such extremely small dimensions, such as those in Fig. 28, which are greatly magnified. It appears much more plausible to assume that, due to the manner in which the atoms are arranged and bound together, certain portions of the crystal face can be dissolved more readily than others. It may, moreover, be pointed out again that the crystallographic axes, which are perpendicular to the cube faces, are the directions in which the atoms are widely spaced and the valence bonds weak. Accordingly, it is suggested that these outlines on the cube faces may well be interpreted as the result of differential solution.

Diamond Dust

The question is often asked why is it possible to saw, grind, or polish the diamond with its own dust. In the light of the foregoing discussion a very definite explanation is possible.

Diamond dust is prepared by crushing a crystal or fragment to fine powder. In the crushing process, due to the excellent octahedral cleavage, small particles with cleavage surfaces result. By following well established procedures, dust of uniform grain size may be obtained. Usually several kinds of dust are prepared which vary from coarse to fine depending upon the size of the particles.

---

[33] *Ibid.*, Plate 23, crystal 61.

[34] Text, p. 220.

The sawing of a diamond is done by means of a small, thin, phosphor-bronze disc which revolves rapidly. The edge of the disc is impregnated with diamond dust and oil. For polishing purposes a horizontally revolving cast-iron plate or wheel called the "skeif" is used. The skeif is somewhat porous. When diamond dust mixed with olive oil is placed upon it, the particles lodge or embed themselves in the pores or pits. In the random distribution of the dust in the saw or skeif, some of the particles will obviously have cleavage surfaces exposed. Since these are the hardest surfaces, such particles are able to abrade the stone in directions of inferior hardness, that is, in those not parallel to the octahedron faces, and most readily in those parallel to a crystallographic axis. As the particles are loosely held they are free to turn or roll and hence new portions will be exposed. Then, too, the fine particles which are removed from the stone during the process assist in the sawing and polishing.[35]

Sawing is best accomplished in directions parallel to the faces of the cube, commonly called the *sawing grain*. Experience shows that it is almost impossible to saw the diamond if the plane of the cut varies more than a few degrees from that of a cube face. Although there are possible sawing grains parallel to the faces of the rhombic dodecahedron, they are not commonly used.

Acknowledgments

We are indebted to Messrs. Lazare and Leo Kaplan of New York City, and Mr. J. Levy of Detroit for information and helpful suggestions on diamond cutting; and to Professor Kasimir Fajans of the Department of Chemistry of the University of Michigan for advice and assistance in the calculation of the valence bonds.

---

[35] Reference 12, p. 62.
Also, for more details, reference 14, pp. 94–95, and 97–99.

IDENTIFICATION OF DIAMOND IN THE CANYON DIABLO IRON

C. J. Ksanda, *Geophysical Laboratory, Carnegie Institution of Washington,*
and E. P. Henderson,* *U. S. National Museum, Washington, D. C.*

The first good evidence of diamond in a known meteorite was published in 1888, by Jerofejev and Lachinov.[1] In a stony meteorite which fell in September 1886, near Novo-Urei, they found grayish grains which were regarded as diamonds. Kunz[2] was able to procure a small piece of the same meteorite and substantiated their conclusion.

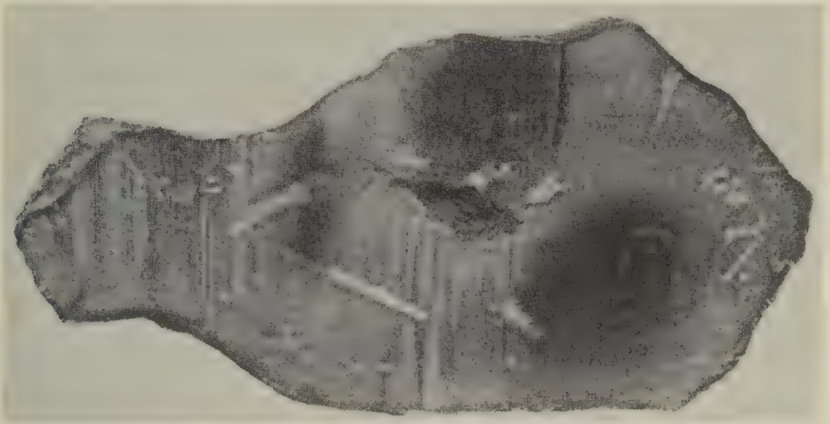

Fig. 1. Section of Canyon Diablo meteorite showing the area in the center of the meteoritic iron from which the diamonds were removed.

In 1891 Foote[3] reported hard particles in the Canyon Diablo iron. Much subsequent work in which the mode of occurrence and general crystallographic appearance of these grains are described, is reviewed by Farrington.[4]

Recently small black grains embedded in a slice from a Canyon Diablo iron have been identified by means of the *x*-ray powder spectrum method and by microscopic examination as diamonds. The specimen containing these diamonds was purchased by the U. S. National Museum from H. H. Nininger, Denver, Colorado, who while cutting the specimen found small dark inclusions that resisted the saw, and assumed that they were diamonds. The section of iron shown in Fig. 1 is 115 mm. long, 55 mm. wide at its widest part, and weighs 411.7 grams. The specimen was not further polished in the U. S. National Museum laboratories because to do so would probably grind away several of the small diamonds visible to the naked eye.

---

* Published by permission of the Secretary of the Smithsonian Institution.

[1] Jerofejev, M., and Lachinov, P., *Zapiski Mineralogicheskoe Obshchestvo*, Leningrad, (2) **24**, 263–294 (1888).

[2] Kunz, G. F., *Science*, **11**, 118–119 (1888).

[3] Foote, A. E., A new locality for meteoric iron with a preliminary notice of the discovery of diamonds in the iron: *Am. J. Sci.* (3), **42**, 413–417 (1891).

[4] Farrington, O. C., *Meteorites; their Structure, Composition and Terrestrial Relations.* By author. Chicago, **1915.**

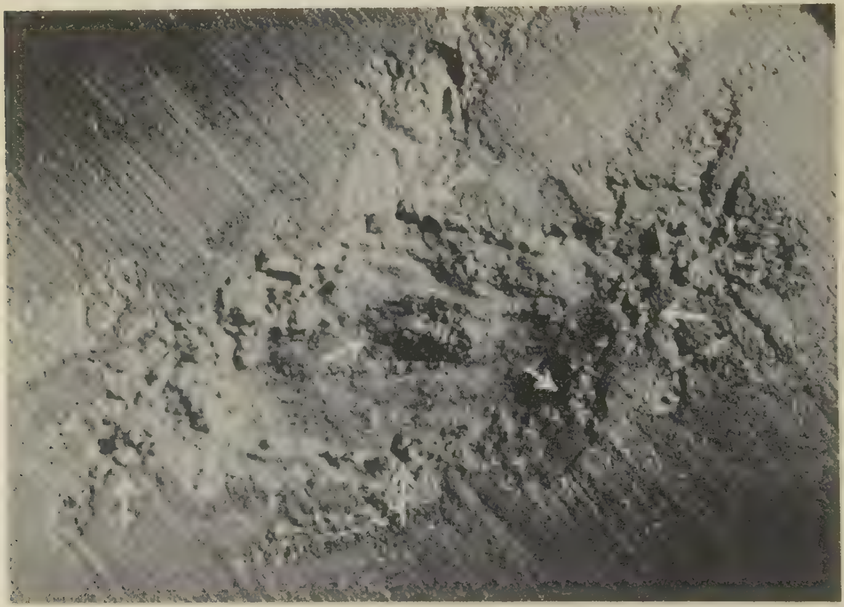

Fig. 2. The cavity enlarged 6×, containing black diamonds, showing larger individuals lining the inner wall, securely embedded in graphite. Arrow points indicate the location of larger grains of black diamonds partly excavated.

The diamonds occur associated with some graphitic material within a troilite area. Immediately surrounding the troilite is a series of irregular areas of schreibersite. A wax dam was constructed around the area and the diamonds were freed by repeated treatments of nitric and hydrochloric acid. The insoluble residue was washed out and saved. This residue was slightly contaminated with some organic matter as the acid reacted with the wax dam. The black grains were repeatedly boiled with mixed acids and the acid soluble portion decanted off and rejected.

About 50 individual black grains were recovered whose sizes vary from 0.1 to 0.6 mm. The cavity made by the acid (see Fig. 2) is lined with larger individuals securely embedded in the graphite and troilite. Several of these black grains were removed by working them out with a needle point. The largest was 0.9 mm. in diameter.

The grains resemble the black diamond, or carbonado, of commerce. Under the microscope they are black, and as recovered are porous, and therefore seem to consist of minute individuals. A rude layering appears in the larger grains. They are more easily broken down than ordinary black diamond.[5]

Grains rubbed between two pieces of ordinary black diamond did not produce any scratches visible with the microscope.

X-ray analysis. Crushed particles were mounted on a fine thread by means of a film of vacuum grease and a photograph was taken with Cu-K radiation in a circular camera of an effective radius of 57.2 mm. The specimen was rotated uniformly during the exposure. The results of the x-ray analysis are given in Table 1. The diffraction pattern shows only the lines theoretically possible within the angle of reflection with Cu-radiation for the cubic lattice of diamond. The systematically absent reflections are characteristic of the face-centered lattice type of diamond. The unit cell dimension, $a_0=3.55_7$, calculated from spacings d/n is in agreement with previously published data.[6]

TABLE 1

Planar spacings and relative intensities of the x-ray diffraction lines of diamond from a rotation powder spectrum taken with filtered Cu-K radiation. Estimated intensities of the diffraction lines are based on a scale of ten, where ten represents the intensity of the strongest line.

Line	Intensity	*hkl*	d/n	a_0
1	10	111	2.062	3.572
2	6	220	1.255	3.550
3	4	113	1.069	3.545
4	1	400	.889	3.556
5	1	133	.817	3.561
				$a_0=3.55_7$

X-ray powder photographs of the graphitic mass were also taken. The resulting diffraction pattern shows a large number of lines,[7] not all of which could be identified. Of the 16 lines measured on the film, only nine are identical in position and intensities with the first nine lines of the known graphite structure.[8] No lines characteristic of diamond were found on these films.

---

[5] Black diamonds (or carbonado) such as those used for industrial purposes consist usually of a very compact mixture of gray to black and translucent white particles in various proportions, intimately intergrown. The individual crystals are of microscopic size, and the structure when fractured is fine-grained.

[6] Wyckoff, R. W. G., *The Structure of Crystals*, 2nd Ed., Chemical Catalog Co., Inc., New York, **1931.**

[7] The specimen appeared slightly altered by previous treatment and etching of the cavity with acid.

Optical properties. Under the microscope, in a melt of sulfur and selenium, most crushed grains were not transparent except in irregular patches at thin edges, where they were isotropic; n for orange colored light is greater than 2.37 and for yellow light about 2.42.[9]

---

[8] See, for example, Hofmann, U., and Wilm, D., *Zeits. f. Elektrochem.*, **42,** 504–522 (1936).

[9] The optical properties were determined by Dr. H. E. Merwin, and his aid in this investigation is gratefully acknowledged.

GRAPHIC GRANITE

Ernest E. Wahlstrom, *Harvard University, Cambridge, Mass.*

Contents

Definitions and history of term........ 681
Texture and composition........ 682
Orientation of quartz in graphic granite........ 685
Origin of graphic granite........ 692
Summary and conclusions........ 697
Acknowledgments........ 698
References........ 698

Definitions and History of Term

Graphic granite is a familiar and abundant constituent of many pegmatites, and unlike most other rocks of igneous origin it possesses certain definite characteristics that permit its ready identification in the field or in hand specimen. All graphic granite, when split in certain directions, shows an interesting structure that suggests crude attempts at writing or printing with a broad pointed pen. Commonly used terms, such as graphic granite, runite, graphic pegmatite, Hebraic pegmatite, and Schriftgranit, are all descriptive expressions designed to emphasize the importance of this most obvious property of the rock.

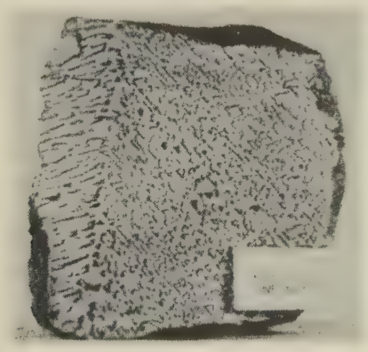

Fig. 1. Graphic granite. Topsham, Maine. The polished surface of the slab shows both transverse and longitudinal sections of the quartz rods. The cleavage of the feldspar extends without interruption through the whole piece—an indication that the feldspar is all part of a single crystal.

The graphic pattern is brought about by the growth in or with feldspar of tapering cross-striated pencils of quartz, which in transverse section generally show one or more reentrant angles and an outline that suggests anything from a stubby boomerang to an awkward attempt to construct the letter "C" with fluted angular rods of lenticular cross-section. Various writers have likened the structures to the runes of the Norsemen, to Hebraic characters, or, with less reason, to the hieroglyphs of the ancient Egyptians. From the last is derived the not uncommonly used word "hieroglyph" as applied to the quartz rods. Fersmann (1928) has coined the word "ichthyoglypts" because of the fancied resemblance of the rods to tailless fish.

Although the term "graphic granite" is well established by usage, it might be a general improvement to use the expression "graphic pegmatite," for the rock is not a true granite, and it probably has not formed by the direct, *in situ*, solidification of molten magma. Rather it has crystallized in a special environment under special conditions. Johannsen (1932) urges the usage of Pinkerton's word "runite." This term has the advantage of being descriptive, and, at the same time, it does not imply a necessary relationship to normal granite.

Graphic granite everywhere is found associated with pegmatites, and its presence serves as a well established criterion for the determination of a rock as pegmatite. As a matter of fact, Kemp (1924) points out that Haüy originally used the word "pegmatite" for a rock that today would unquestionably be called graphic granite. As the term "pegmatite" was gradually adopted, its application was extended, so that it eventually attained its present implications, and graphic granite came to be regarded merely as a variety of pegmatite.

Texture and Composition

The two essential minerals of graphic granite, quartz and feldspar, have highly contrasting ranges in size. Inasmuch as the quartz generally appears to be embedded in feldspar, the masses of feldspar generally are larger than the quartz grains. Individual grains of feldspar in megascopic intergrowths rarely have diameters less than a centimeter and commonly are several centimeters across. In some places graphic intergrowths are present in continuous feldspar crystals that attain as much as two or three meters in width. In contrast, quartz rods show a rather limited range in size. The rods may in exceptional rocks reach a length of ten or twelve centimeters, or greater, and a diameter of two or three centimeters. Typically, however, the rods are smaller and range downward in dimensions to sizes that are almost imperceptible to the unaided eye.

In general, if the rods, or "ichthyoglypts," are not large enough to be detected in the hand specimen, the rock cannot properly be called graphic granite. For the graphic aggregates that are observed under the microscope a whole suite of terms has been devised, including such familiar words or expressions as, micropegmatite, myrmekite, micrographic intergrowth, symplektite, granophyr, etc. Although many microscopic structures are very suggestive of the megascopic features of graphic granite, there is no necessary implication that the processes of formation are the same. For example, micrographic granite or granophyr is a common but minor constituent in diabase, whereas graphic granite is ordinarily associated with more felsic rocks. However, a study of the genesis of the microscopic intergrowths probably will throw light on the perplexing queston of the origin of the large scale features seen in hand specimens.

The mineral composition of graphic granite is comparatively simple. Only two essential minerals are present, namely, quartz and feldspar. The quartz may be colorless, smoky or milky and, according to Fersmann (1928), may be of either the "high" or "low" varieties. Fersmann (p. 88) notes that an individual rod may contain both high- and low-quartz. This condition obtains in certain pegmatitic cavities where the high-quartz in the walls passes into crystallized low-quartz in the cavities. The low-quartz crystals commonly protrude from feldspar crystals, which serve as a host for the quartz. It is thought that the difference in the two varieties of quartz is proof of lowering temperatures during the period of formation of the pegmatite.

The present writer has etched half a dozen polished specimens of quartz from graphic intergrowths and has found no evidence indicating positively that the quartz in these particular specimens is either of the high or low varieties. In any event, without crystals, many of the criteria for the determination of the temperature of formation of the quartz are of very doubtful value, and a positive distinction between the two varieties is in many rocks fraught with difficulty and uncertainty.

The quartz in cavities is crystallized, and where it is present with feldspar, it not uncommonly appears to lie on or protrude from crystals of the feldspar. In these crystals the quartz ordinarily extends into the feldspar as stubby cross-striated polygonal "roots," which within a few millimeters take on all of the aspects of quartz rods in ordinary graphic granite. In order to see the graphic structure in a crystal of feldspar, it is usually necessary to break the crystal open; quartz rarely appears in a graphic pattern on the surface of a feldspar crystal.

Where quartz and feldspar crystals make contact, it is generally observed that the crystal faces of the quartz lose their identity. The feldspar, however, may retain its crystal outline, and in many intergrowths the feldspar is partly or entirely euhedral. In many quartz-feldspar aggregates the contacts are striated polyhedral surfaces, the planes of which do not appear to be related to crystal directions in either of the minerals. The striations are not an expression of twinning, but, rather, are probably the result of a nearly equal struggle for space by the growing minerals.

The most abundant feldspar in graphic granite is microcline microperthite. Orthoclase is often reported in the literature, but none was observed in the specimens studied by the present writer. Some thin sections contain a feldspar that in general appearance closely resembles orthoclase; however, the optics determined with a universal stage indicate that the mineral is microcline. It is possible that most of the so-called orthoclase in graphic granites is in reality microcline.

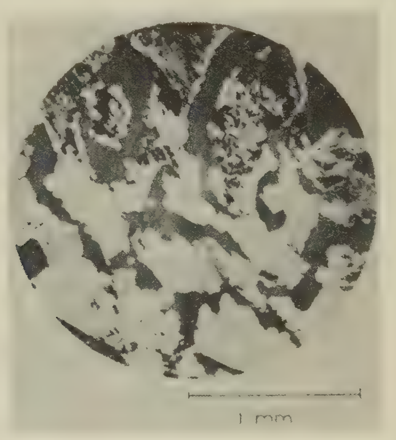

FIG. 2. Photomicrograph of albite graphic granite showing microcline being replaced by albite. Note corrosion of quartz by albite. Albite is white; quartz, medium gray; and microcline, dark gray. Redstone, N. H.

Albite, containing some calcium, is almost universally present in graphic granites. Part of the albite is believed to have formed by exsolution and is the familiar plagioclase in perthite and microperthite. However, many graphic granites contain abundant introduced albite, or albite-oligoclase, which has partly or completely replaced the microcline. Residual patches of microcline and embayed or corroded quartz rods in many graphic granites support the conclusion that the replacing plagioclase is generally later than both microcline and quartz. In some specimens all stages of replacement are visible, and, as an extreme result, all of the microcline is removed. Rocks displaying such features might properly be called "albite graphic granite." It is here suggested that most of the so-called "oligoclase graphic granites" are nothing more or less than replaced ordinary microcline graphic granites.

Many writers have stated that the ratio of quartz to feldspar is constant in graphic granite. For example, Holmes (1914) found that certain graphic granites in Mozambique showed a range of 24.2 to 27.9 per cent of quartz by weight. Vogt (1930) insists that the amount of quartz in microcline graphic granite is near 26 per cent and is definitely confined within limits ranging from 23 to 28 per cent by weight. He believes the amount of quartz in oligoclase graphic granite falls within the limits 33 to 38 per cent by weight. However, it should be stated that many workers, either by direct statement or implication, particularly in North America, do not subscribe to Vogt's ideas, and consider the quartz-feldspar ratio as variable beyond these limits. Among those who do not support the idea of a fixed ratio are Landes (1932), Hess (1933), Schaller (1933), Fenner (1926), Bastin (1911), and Bygden (1906).

Orientation of Quartz in Graphic Granite

The question of whether or not the quartz in graphic intergrowths is definitely oriented with respect to the feldspar is of prime interest in the solution of the problem of the origin of the structure. If it is a fact that the quartz is everywhere definitely oriented, a strong point is gained in favor of a theory of simultaneous crystallization. Among the most important works on the subject of regular intergrowth of quartz and feldspar are two papers by Fersmann (1915 and 1928). The earlier paper was in Russian and, because of this, was not readily accessible to most readers of geological literature; the second paper was in German, and contained not only the substance of the first paper but, in addition, a review of progress by Fersmann and others in the period between the two papers.

Fersmann states that 88 per cent of all the specimens of graphic granite that he has examined are characterized by the growth of the quartz in such a manner that one of its trapezohedron zones coincides with the prism zone of the feldspar. Thus is brought about the parallelism of the prism edges of the feldspar and an edge between two adjacent rhombohedron faces of the quartz. This supposed coincidence is called the trapezohedral law (or as termed by many other writers, "Fersmann's law") and shows several modifications, all of which possess one property in common, that is, in each the *c* axis of the quartz makes an angle of 42°16′ with the *c* axis of the feldspar. The modifications of the law are graphically portrayed by the points on the small circle in Fig. 3, which shows the points of emergence of the *c* axis of quartz on a stereographic projection perpendicular to the prism zone of the feldspar. Figure 3 also shows the orientations of quartz according to other laws as described

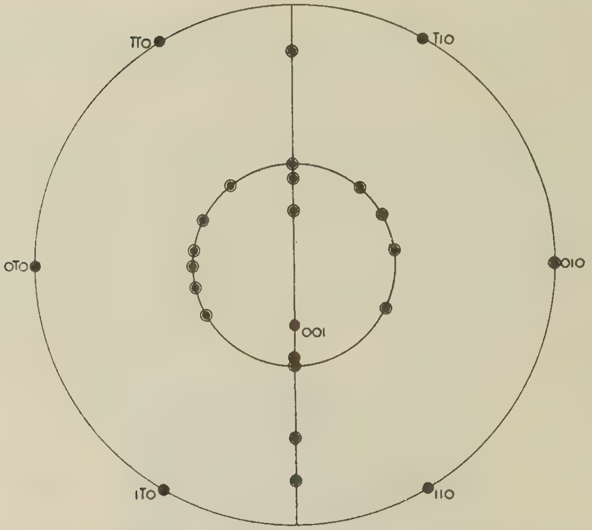

FIG. 3. Stereographic plot showing points of emergence of *c* axis of quartz. Plane of projection is perpendicular to the *c* axis of the feldspar. Modifications of the trapezohedral law are indicated by the double circles in the inner small circle of *rho* equal to 42°16′. Other laws are indicated by the points lying within or without the inner circle. After Fersmann (1928).

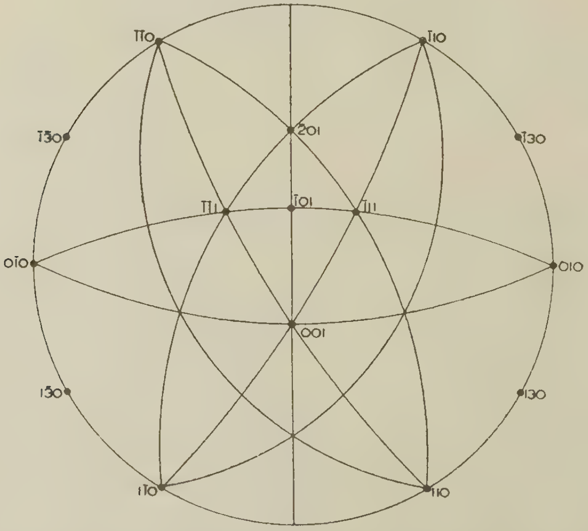

FIG. 4. Stereographic projection of orthoclase showing important faces and zones.

by various writers. Laws other than the trapezohedral law are included in 12 per cent of the specimens Fersmann examined.

Visualization of the modifications of the trapezohedral law is aided by the use of stereographic projections of quartz and feldspar in appropriate orientations. A diagram of orthoclase serves equally well for microcline, because the two minerals, although crystallizing in different systems, are very similar morphologically. Figure 4 is a projection of quartz on its trapezohedral zone. If one of these projections is drawn on transparent paper, placed on the other, and rotated about the common center, it will be seen that at intervals certain zones of the two minerals come into approximate coincidence. Each coincidence is described by the position of the point of emergence of the *c* axis of the quartz on a small circle of *rho* 42°16′.

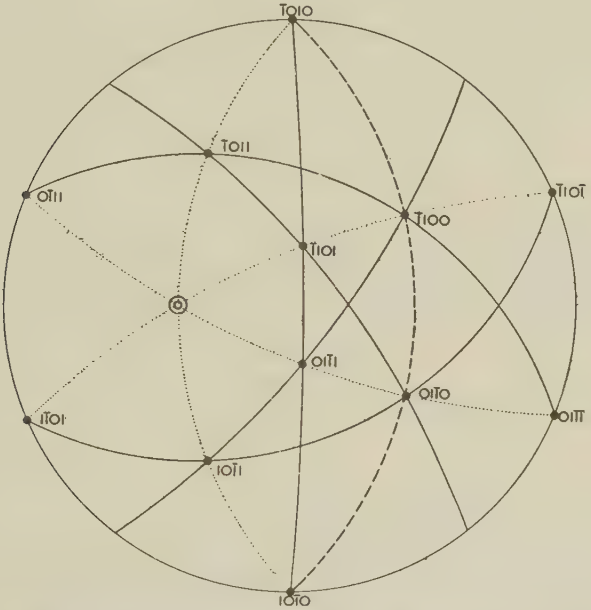

FIG. 5. Stereographic projection of quartz on its trapezohedral zone. The double circle indicates the point of emergence of the *c* axis. Solid lines are the trapezohedral zones; dashed line is the prism zone; and the dotted lines lie in the principal sections of the quartz and are zones including a rhombohedron and a prism face. After Fersmann (1928).

Schiebold (1927) has tested Fersmann's conclusions by comparing the atomic structures of quartz and feldspar. He states that the atomic groupings of the two minerals are in many respects similar, and he accepts Fersmann's conclusions as valid. In a later publication (1930)

Spangenberg and Neuhaus concur with Schiebold and Fersmann, but Schiebold's structure for feldspar was shown to be wrong by Taylor (1933).

In order to test the validity of Fersmann's law, the present writer assembled and studied a representative suite of graphic granites from the collections in the mineralogical laboratories of Harvard University. Specimens were chosen more or less at random and included samples of material from several localities in Colorado, California, Connecticut, New Hampshire, Maine, Japan and Portugal. Thin sections of thirty of these specimens were examined on a universal stage, and the relative orientations of the crystallographic directions of the quartz and feldspar were determined from their optics by the usual means.

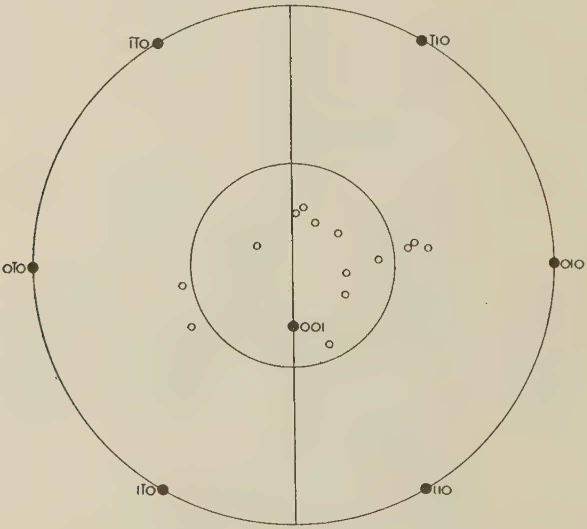

FIG. 6. Plot of graphic granite from Auburn, Maine, showing points of emergence of *c* axis of quartz (small circles) on a stereographic projection of orthoclase. All the orientations are present in a single thin section of feldspar of uniform orientation. Points determined with a universal stage.

Another, more direct, method of study was the measurement with a contact goniometer of numerous well crystallized intergrowths of quartz and feldspar from the extensive Bello Portuguese collection at Harvard. Almost without exception the studied specimens from this collection show graphic intergrowths in the basal portion of the feldspar crystals, and from a study of thin sections of these crystals, it was observed that, in general, most of the quartz in the graphic intergrowths is connected

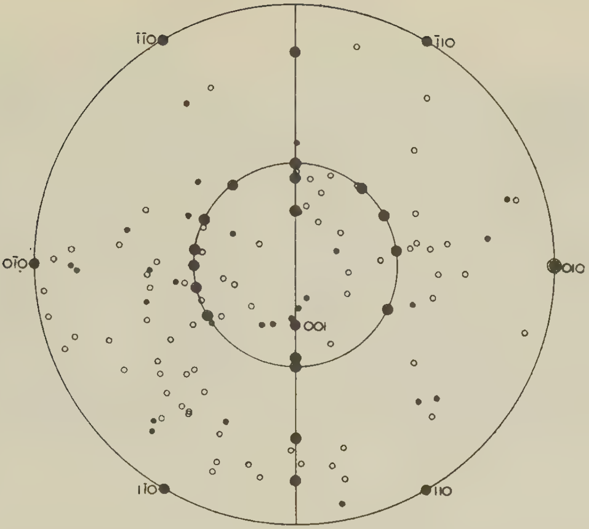

FIG. 7. Points of emergence of the *c* axis of quartz on a stereographic projection of feldspar. The solid circles represent measurements with a contact goniometer, and the hollow circles indicate the results of measurements with a universal stage. The double circles indicate the points of emergence of the *c* axis of quartz according to Fersmann and other writers.

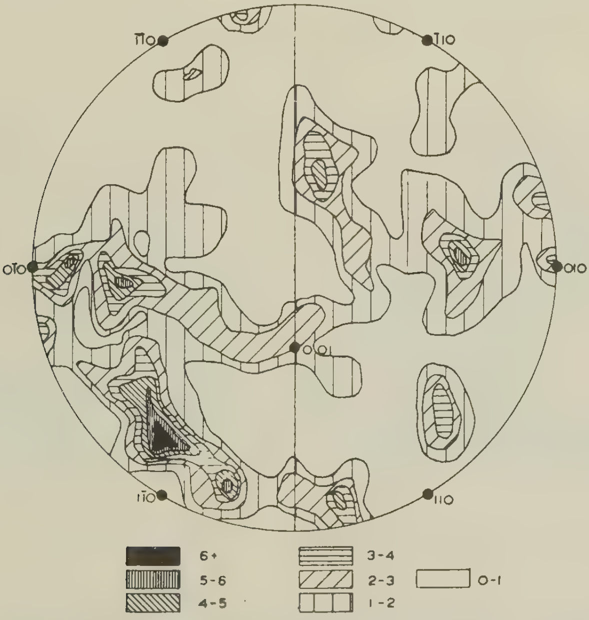

FIG. 8. Stereographic projection perpendicular to the prism zone of feldspar showing by percentage contours the distribution of the points of emergence of the *c* axes of quartz. The points in Fig. 7 were plotted on an equal-area net and contoured according to the technique suggested by Ingerson (1938).

with and has the same orientation as the crystals protruding from the sides and tops of the feldspar crystals.

The combined results of a hundred measurements with the universal stage and contact goniometer are shown in Figs. 7 and 8. Figure 8 is a variation of the plot in Fig. 7 and is designed to show by contours the nature of the distribution of the *c* axes of quartz on an equal-area stereographic projection in the prism zone of the feldspar. An examination of either Fig. 7 or 8 shows that there is no consistent orientation of the quartz in the feldspar. This is in direct contradiction of the views expressed by Fersmann and others as outlined in preceding paragraphs. It should be especially noted that what minor concentrations are present are not on or near the small circle that marks the positions of emergence of the *c* axis of the quartz as demanded by the "trapezohedral law."

Because of certain errors inherent in the technique of universal stage measurement, the results as shown in the stereographic plots cannot be regarded as exceedingly accurate. However, an allowance of plus or minus three degrees in any direction should take care of all errors of observation. But even with such an allowance there is no basis for an assertion that the quartz is consistently oriented with respect to the feldspar.

In crystallographic usage the term "law," as applied to twins and other variations of crystal growth, generally signifies a definite geometrical relationship between different portions of a crystalline substance. The exact nature of the growth depends on several factors such as the environment during and subsequent to the formation, composition, etc. However, when twins or other crystal variations develop in accordance with one law or another, certain space relations must obtain. If these conditions are not rigidly fulfilled, the substance in question cannot be said to have grown in accordance with a specific law.

A statistical study of hundreds of graphic intergrowths of quartz and feldspar might show a tendency for the quartz rods to repeatedly favor certain directions in the feldspar, but unless the crystallographic directions are sharply defined by specific mutual angular relations, the intergrowths cannot be regarded as conforming to specific laws. The present investigation is not comprehensive enough to determine whether or not quartz statistically favors any particular direction or directions in the feldspar, but it does indicate that the relations probably do not conform to the requirements of a definite set of crystallographic laws.

One of the strongest arguments in favor of crystallographic control of the quartz by the feldspar is the common observation that adjacent quartz grains show simultaneous extinctions over broad areas in thin sections. This argument is particularly compelling when it is demon-

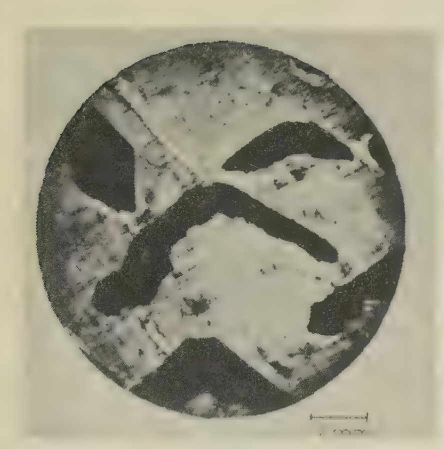

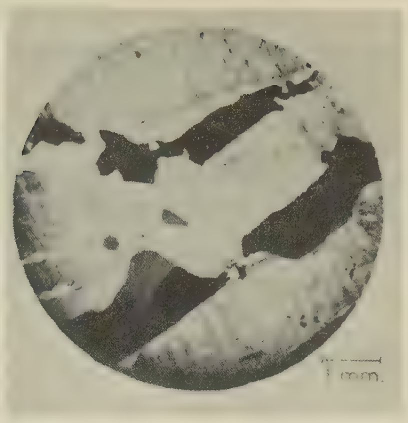

Fig. 9. Photomicrograph of graphic granite showing uniform orientation of quartz rods. Crossed nicols. Auburn, Maine.

Fig. 10. Photomicrograph of graphic granite showing non-uniform orientation of quartz within individual rods. Crossed nicols. Auburn, Maine.

strated that the quartz is present in a series of separate rods that do not interconnect. The idea that the simultaneously extinguishing patches are of necessity parts of a single branching or anastamosing crystal has been shown repeatedly to be erroneous.

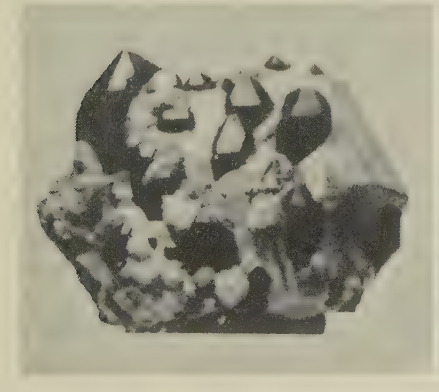

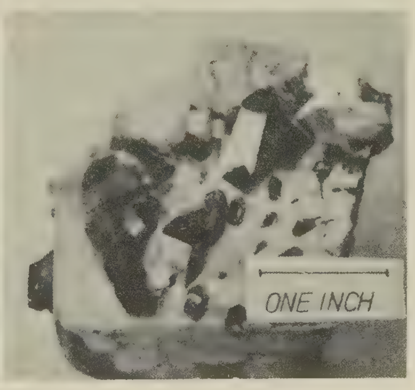

Fig. 11. Parallel growth of smoky quartz crystals in an aggregate of non-uniformly oriented feldspar crystals. The quartz forms graphic pencils within the feldspar crystals. $\frac{2}{3}$ natural size. Laboreiro, Portugal.

Fig. 12. Microcline crystal showing several differently oriented smoky quartz crystal groups. The quartz forms graphic pencils within the feldspar. None of the quartz crystals are oriented according to the requirements of the trapezohedral law. Serra Castro, Laboreiro, Portugal.

Most thin sections of graphic granite actually do show simultaneous extinction of quartz grains over the whole field of view under the microscope. However, some sections contain several rods of different orientation, and it is not unusual to observe several grains of decidedly different orientation within a single rod of quartz; parts of adjacent single rods may extinguish simultaneously over a section. The simultaneously extinguishing rods commonly are present in single crystals of feldspar, and, in general, the complexity of orientation of the quartz increases with a decrease in the size of the feldspar grains. But some complex aggregates of feldspar crystals are cut cleanly across by a group of parallel quartz individuals. In other words, parallelism of the quartz rods is not dependent on the relation to the feldspar host.

Despite the complexities of orientation as outlined above it is probable that in certain localities graphic quartz does show a fairly constant orientation in some particular direction or directions in the feldspar. As a matter of fact, it would be strange if this were not so because of the laws of chance; but the data at hand seem to indicate that intergrowths of quartz and feldspar according to a geometric law are the exception rather than the rule.

ORIGIN OF GRAPHIC GRANITE

Fersmann states that the regular intergrowth of quartz and feldspar proves the theory of simultaneous growth of these minerals. Schaller (1926) suggests that the quartz rods have formed by replacement and tend to follow zones of weakness, such as cleavage planes and twinning planes. However, many investigators have shown that the quartz rods do not necessarily follow such planes, but develop with no regard for these structures. Landes (1933) offers the theory that replacement may be controlled by the lattice structures of the host and guest minerals so as to give graphic structures.

Vogt (1930 and 1931) vigorously supports Fersmann's contentions and offers what he regards as additional proof of simultaneous crystallization. He examined suites of feldspar specimens showing "oriented' graphic granite and observed many feldspar individuals containing a core of feldspar sharply separated from wholly or partly enclosing layers of graphic granite. The feldspar in the core has the same orientation as that in the graphic intergrowth and is commonly separated from it by a sharp boundary plane, which parallels a possible crystal face. In general, the quartz rods are nearly, or quite perpendicular to the plane of contact. The most important bounding planes are (010), (001), (110), and ($\bar{2}$01), although other planes are locally important. These observations by Vogt appear at first glance to substantiate the conclusions drawn by

Fersmann as to the manner of development of the quartz rods or "ichthyoglypts" in graphic growths. Fersmann believes that the quartz rods grow at right angles to "induction faces" (important crystal faces) in the feldspar. The same phenomenon has been described by other writers, as for example, by Brögger (1881) and Mäkinen (1913).

Figures 13 and 14 are based on two of Vogt's photographs of "oriented graphic granite" (1930 and 1931). The original specimens came from Hitterø and Norestø in Norway and were chosen for illustration because Vogt regarded them as proof of this theory of the cotectic crystallization of the quartz and feldspar in graphic granite. But such specimens are probably exceptional, and it is a simple matter to find specimens that do not conform to Vogt's ideas. For example, Fig. 15 is a photograph of a polished section of the interior of a feldspar crystal from Nuevo, California. The crystal consists of a core of microcline surrounded in turn by a layer of graphic granite and an outer layer of microcline. The side pinacoidal cleavage extends without interruption through the entire crystal. The described features may be explained as the result of replacement of a favorable layer in a zoned crystal, or as alternate deposition of feldspar and graphic granite. Neither of these explanations supports Vogt's assertions, and merely serve to show that conditions are not as simple as Vogt supposed.

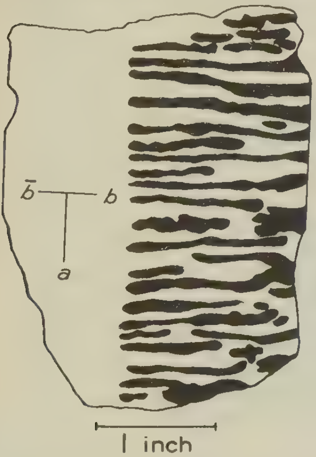

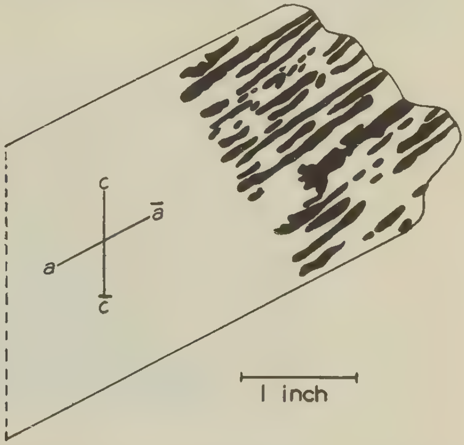

FIG. 13. Sketch to show nature of quartz-feldspar intergrowths in "oriented graphic granite." Rods of quartz (black) are approximately perpendicular to 010 plane of feldspar. Section cut parallel to 001. Based on a photograph by Vogt (1931, p. 200) of a specimen from near Norestø, Norway.

FIG. 14. Sketch to indicate nature of quartz-feldspar intergrowths in "oriented graphic granite." Rods are nearly perpendicular to $\bar{2}01$ plane in feldspar. Based on a photograph by Vogt (1930, p. 109) of a specimen from near Hitterø, Norway.

Vogt's views (1930) may be expressed tersely in his own summary, which follows:

> "1. Fersmann's crystallographical investigations decisively prove the simultaneous primary crystallization.
>
> "2. The investigations concerning the oriented graphic" (Vogt's investigations) "demonstrate the same conclusion. By two different working methods, quite independent of each other the simultaneous crystallization is thus now established.
>
> "3. Further, we point out that the quantitative proportion between quartz and feldspar (microcline) varies only within narrow limits."

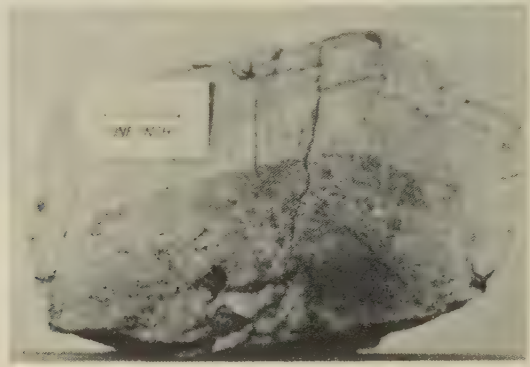

FIG. 15. Polished section through a microcline crystal from Nuevo, California. The crystal has a core of pure feldspar surrounded by a layer of graphic granite, which, in turn, is surrounded by a layer of feldspar. The section is cut parallel to the side pinacoid of the feldspar. The feldspar forms a single crystal as shown by the fact that the 010 cleavage extends without a break through the whole mass.

Vogt rejects as erroneous any theories involving the concept of replacement and, in particular, attacks the views held by Schaller and by later workers stimulated by Schaller's observations.

The idea that quartz and feldspar are precipitated simultaneously suggests the action in artificial binary or ternary systems where, under certain conditions, eutectic and cotectic conditions prevail. Vogt regards graphic granite as a result of precipitation along a cotectic curve in an essentially ternary system consisting largely of quartz, potash feldspar with some albite (and a little anorthite), and containing small amounts of Fe_3O_4, mica components, water, etc.; he regards as a probable constituent of the system a compound represented by the formula $SiO_2 \cdot nH_2O$. Vogt finds it necessary to postulate the last named component in order to explain the fact that again and again large amounts of massive quartz are present in the central portions of pegmatite dikes—an observation which would tend to nullify the conclusion that graphic granite forms as a cotectic mixture, if it could be proved that the late quartz existed in solution as such. It is assumed that the component $SiO_2 \cdot nH_2O$ breaks down upon cooling and gives "free quartz" and water. In other words, in considering the origin of graphic granites, Vogt places much significance on the presence of a hypothetical compound in the pegmatitic solutions.

As has been demonstrated in the present paper, quartz in graphic growths is not ordinarily consistently oriented with respect to feldspar. However, this conclusion does not necessarily disprove the theory of simultaneous crystallization, but, rather, it calls for a revaluation of the data used to support this theory. At the same time necessity arises for a consideration of the theory of the replacement origin of graphic granites, so that the opposing theories may be balanced against each other in the light of the new data.

The writer feels that it is very difficult to distinguish positively between structures produced by simultaneous growth and replacement. Without doubt replacement is entirely capable of producing the same features as simultaneous growth, for crystal forces will be similar in either process. There seems to be no obvious reason for stating that the forces interplaying between quartz and feldspar during contemporaneous concomitant growth are not almost, if not exactly, the same as those active during replacement of the feldspar by quartz. The final explanation of the origin of a specific deposit must accordingly, be based on all available evidence and must include a careful consideration of both field and laboratory evidence. Accumulated observations will probably demonstrate that graphic granite can form as a result of either simultaneous crystallization or replacement.

Fairly positive evidence that the quartz has been introduced is found in graphic granite masses closely associated with cross cutting veins or lenses of massive quartz. However, as pointed out above, Vogt (1930) regards the massive quartz as residual from the breakdown of hydrated silica. In such examples conclusions based on field evidence probably are valid and are more trustworthy than data gathered from hand specimens or thin sections.

The proponents of the theory that all graphic granites form by replacement must answer the question as to what does actually happen when quartz and feldspar do develop simultaneously. Significant information bearing on this question may be found in cavities in pegmatite where individual crystals of quartz and feldspar come into contact with each other. The surface of contact duplicates the contact of graphic pencils with the surrounding feldspar. The surface of contact, then, is identical whether the quartz develops entirely within a crystal of feldspar or whether single adjacent crystals of the two minerals interfere during growth. Crystals of quartz resting on feldspar almost invariably extend into the feldspar as irregular roots, which give rise to a typical graphic structure within the crystal. It is more logical to assume that the quartz and feldspar grew simultaneously than to assume that late quartz developed crystals on the surface of the feldspar crystal and at the same time, sent a long pencil-like root into it by replacement. However, crystal lined cavities are special features of pegmatites and occupy only a fraction of a per cent of the bulk of most pegmatites.

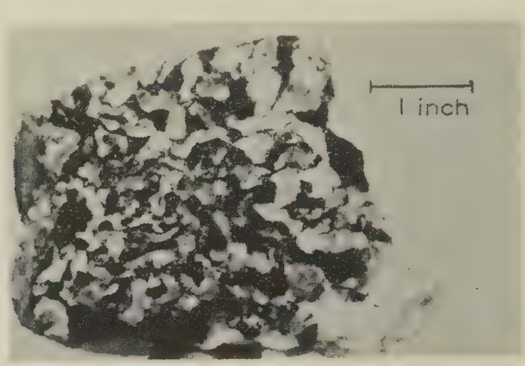

FIG. 16. Graphic intergrowth of quartz and back tourmaline. Portland, Connecticut.

Megascopic graphic intergrowths of quartz with minerals such as tourmaline, garnet, hornblende and muscovite are present in some pegmatites and possess many of the properties of ordinary graphic granite. As in graphic granite, there is no evidence of a fixed proportion of one mineral to another, and it is very unlikely that pairs of minerals were precipitated simultaneously along a cotectic curve. Quartz-tourmaline intergrowths from Portland, Connecticut, and Auburn, Maine, probably formed by tourmaline replacement of quartz (Fig. 16). However, a thin section of quartz and hornblende in graphic intergrowth provides evidence indicating that the quartz is younger than the hornblende. These examples suffice to demonstrate that quartz, either by replacing or by being replaced, can form graphic textures, and provide an excellent argument for the replacement origin of graphic granite.

Selective replacement of the feldspar in graphic granite by late pegmatitic minerals produces interesting features. For example, graphic intergrowths of quartz and muscovite from Auburn, Maine, and Amelia Court House, Virginia, are reasonably interpreted as selective replacements of microcline in ordinary graphic granite by later muscovite.

The writer has examined many pegmatites in the broad pre-Cambrian terranes in the Front Range of Colorado and believes that most of the widespread and abundant graphic granites he has examined there have formed by replacement of massive microcline by quartz, which gained access through fractures or complex zones of weakness. But it is quite possible that many of the graphic structures in the walls of cavities in the well known pegmatites in the Pikes Peak and other regions in Colorado represent simultaneous intergrowths.

Inasmuch as graphic granites are very similar the world over, it is reasonable to assume that the processes active in one place are active in another. But too strong adherence to a single theory of formation may lead to broad generalizations that do not conform to all the facts for a given deposit. The writer believes that quartz replacement in feldspar is the dominant process in graphic granite formation, but at the same time, believes that simultaneous growth is locally important.

Summary and Conclusions

A study of megascopic graphic intergrowths of quartz and feldspar from many localities indicates that, in general, the geometric relations between the two minerals do not conform to the requirements of any crystallographic law or laws of growth; that is, the quartz in graphic granites does not show any constant orientation with respect to the feldspar. Most quartz crystals resting on microcline are connected with and have the same orientation as graphic quartz rods within the feldspar. Quartz in graphic granite commonly is present in groups of separate parallel rods; however, adjacent rods may or may not have the same optical orientation, or individual rods may contain several grains of random orientation. Groups of parallel rods generally are confined to single crystals of feldspar, but in some specimens the rods cross the boundaries between adjacent feldspar grains. The *c* axis of the quartz may or may not be parallel to the long direction of a rod.

Selective replacement of the microcline in graphic granite results in the formation of graphic intergrowths of such pairs of minerals as quartz and albite, quartz and muscovite, etc. However, graphic intergrowths of quartz with such minerals as tourmaline, hornblende and garnet probably are produced either by partial replacement of the quartz or by the action of silica-rich solutions on older minerals.

Graphic granite probably forms either by the partial replacement of feldspar or by the simultaneous growth of quartz and feldspar. Most graphic granite appears to have formed by partial replacement of massive microcline by quartz from silica-rich solutions which were guided by fractures or complex zones of weakness in the feldspar. Too strict adherence to one or the other of the opposing theories of origin may lead to erroneous interpretations of field and laboratory data.

Acknowledgments

The writer wishes to express his deep appreciation of the assistance and advice generously given him by Professor Charles Palache, who suggested the problems herein discussed and gave the writer free access to the extensive collections at Harvard University. Professor E. S. Larsen and Dr. Harry Berman, both of Harvard University, read the manuscript and offered many helpful suggestions and criticisms. The writer, however, assumes full responsibility for any errors of observation or judgment that may appear in this report.

References

Bastin, E. S., Geology of the pegmatites and associated rocks of Maine: *U. S. Geol. Survey, Bull.* **445** (1911).

Brögger, W. C., Pegmatitgangene Ved Moss: *Geol. Fören. Förh.*, **5**, 341 (1881).

Bygdén, A., Über das quantitative Verhältniss zwischen Feldspat und Quarz in Schriftgraniten: *Bull. Geol. Inst. Univ. Upsala*, **7**, 1–18 (1906).

Fenner, C. N., The Katmai magmatic province: *Jour. Geol.*, **34**, 673–771 (1926).

Fersmann, A. E., On the graphic texture of pegmatites and its causes: *Bull. Acad. Sci. U.S.S.R.*, 1211–1228 (1915). (In Russian)

———, Die Schriftstruktur der Granitpegmatit und ihre Entstehung: *Zeits. Krist.*, **69**, 77–104 (1928).

Hess, F. L., Pegmatites: *Econ. Geol.*, **28**, 447–462 (1933).

Holmes, A., The pre-Cambrian and associated rocks of the District of Mozambique: *Quart. Jour. Geol. Soc.*, **74**, 31–98 (1919).

Johannsen, A., *Petrography*, Pt. **II**, Univ. of Chicago Press, 84–91 (1932).

Kemp, J. F., The pegmatites: *Econ. Geol.*, **19**, 699 (1924).

Landes, K. K., The Baringer Hill, Texas pegmatite: *Am. Mineral.*, **17**, 381–390 (1932).

———, Origin and classification of pegmatites: *Am. Mineral.*, **18**, 33–56 and 95–103 (1933).

Mäkinen, E., Die Granitpegmatit von Tammela in Finland: *Bull. Comm. Geol. Finl.*, **35**, 28 (1913).

Schaller, W. T., Mineral replacements in pegmatites: *Am. Mineral.*, **12**, 59–63 (1926)

Schaller, W. T., Pegmatites, ore deposits of the Western States (*Lindgren Volume*), Chap. III, Pt. **IV**, 144–151 (1933).

Schiebold, E., Über den Feinbau der Feldspate: *Fortschr. d. Min.*, **12**, 78 (1927).

Spangenberg, K., and Neuhaus, A., Kunstlich gefarbte Kristalle als beispiele sogennanter anomaler Mischkristalle und ihre mineralchemische Bedeutung: *Chemie der Erde*, **5**, 438–523 (1930).

Taylor, W. H., The structure of sanidine and other feldspars: *Zeits. Kirst.*, **85**, 425–442 (1933).

Vogt, J. H. L., The physical chemistry of the magmatic differentiation of igneous rocks: *Skrifter Utgitt av Det Norske Videnskaps-Akademie i Oslo, I Mat. Naturv. Klasse*, 103–130 (1930).

———, Die Genesis der Granite physikochemisch gedeutet: *Zeits. Deut. Geol. Gesells.*, **83**, 193–214 (1931).

SILICIFIED WOOD IN DOLOMITE

JULIAN D. BARKSDALE

INTRODUCTION

There is exposed on the west side of the Sonoma Range, south of Winnemucca, Nevada, a series of folded and faulted sedimentary rocks of Triassic age. The general geology of the area has been studied for several summers by members of the Stanford University field course in geology, and a preliminary report dealing with the structure and stratigraphy is now in preparation.

The youngest Triassic formational unit exposed in the Range consists of a series of interbedded buff, red and green shales, buff sandstones and gray to black limestones and dolomite beds. A shallow water pelecypod fauna, including *Alectryonia sp.*, and *Myophoria whatleae* is closely related to a Mediterranean-Alpine assemblage of Upper Triassic age. Pieces of a jet black siliceous rock were found scattered over the surface of the formational outcrop during the field mapping. Dr. Siemon W. Muller first recognized this material as organic in origin. Subsequently a number of specimens were collected from this and other carbonate beds in the series. The largest piece of wood found was approximately six feet long and eighteen inches in diameter. Most of the preserved specimens are stems or small logs that floated out in the shallow sea, became waterlogged and sank into the carbonate ooze.

Adams[1] has described a piece of wood picked up as float in which the replacing mineral is in part dolomite, but he knew nothing of the origin of the specimen, beyond the fact that it was found in the Midway oil field, Kern County, California. Wieland[2] mentions the occurrence of beautifully preserved calcified wood from the Genundewa limestone, lower upper Devonian, of western New York. The occurrence of silicified fossils in carbonate rocks is not exceptionally rare, but the occurrence of silicified wood in dolomite is unique insofar as the author has been able to ascertain from a search of the literature.

DESCRIPTION OF SILICIFIED WOOD

Some of the petrified wood, in hand specimen, is very fine grained, although not cherty in appearance. Other specimens resemble a medium grained black quartzite. The preserving medium in all specimens is predominantly granular quartz; some sections show minor amounts of the chalcedonic variety. The crystal growth in the fine grained material

---

[1] Adams, S. F., A replacement of wood by dolomite: *Jour. Geol.*, **28,** 356–365 (1920).

[2] Wieland, G. R., The Cerro Cuadrado petrified forest: *Carnegie Institution of Washington,* Publication No. **449,** 62 (1935).

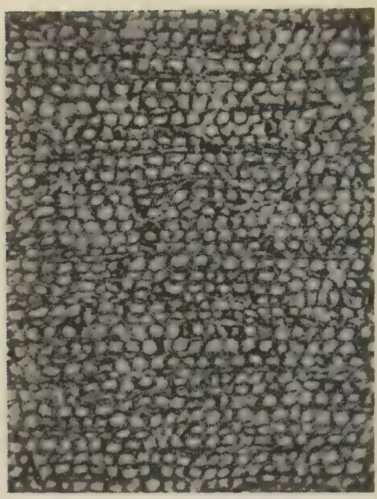

1*a*

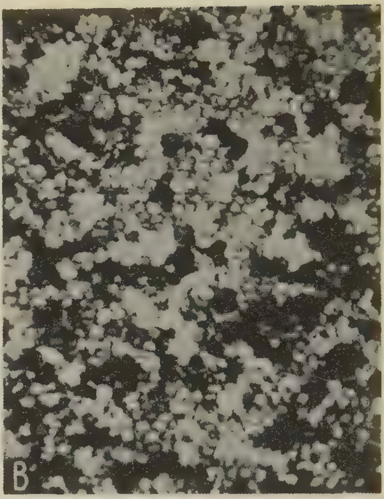

1*b*

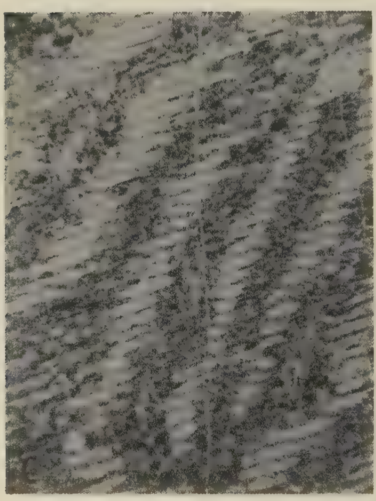

2*a*

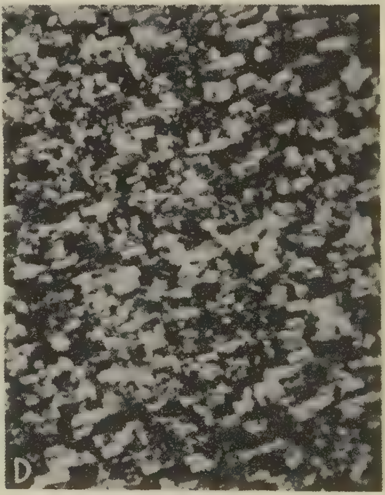

2*b*

FIG. 1*a*. Transverse section of silicified *Araucarioxylon sp.* ×31.

FIG. 1*b*. Crossed nicols. Illustrating the predominantly hyperblastic structure of the preserving quartz. ×27.

FIG. 2*a*. Almost true radial section from same specimen as shown in 1*a*, showing preservation of bordered pits on the tracheid walls. ×31.

FIG. 2*b*. Crossed nicols. Illustrating the influence of the cell walls on the crystallization of many of the quartz grains. ×27.

was influenced by the cell walls as shown in Fig. 2*b*. Single anhedrons may occupy one cell or may include several. In some portions of the slides one can see the primary wall still preserved; in others most of the middle lamella has disappeared, and its place is taken by quartz deposited in optical continuity with the tracheid cell filling. Storz,[3] in his description of Egyptian petrified woods, classifies this type of silicification as *durchkieselung*, simple tracheid filling as *einkieselung*. Where one crystal occupies a single cell the structure is called *oligoblastic;* where the anhedron takes in several cells and cell walls it is called *hyperblastic* (Fig. 1*b*).

There are small areas in some of the thin sections of the coarse grained material showing preservation very similar to that just described for the fine grained material. However, most of these thin sections show a different type of petrifaction. A crude cellular structure has been formed in the coarse grained material where crystallizing subhedral grains of quartz have attempted to clear themselves of the carbonaceous cellular material of the original wood along definite crystallographic directions, and have concentrated the black material just inside their borders. Some of the areas show the original cells to have been distorted by the force of the growing crystals. Other places in the section show well preserved fragments of cellular wood inclosed within a singular anhedral crystal. Some of the cleared areas are single anhedrons; others are made up of several wedge-shaped individuals which have grown outward from centers. Each wedge has forced the carbonaceous material outward to meet or almost meet the black material being forced away from the center of an adjoining grain or group of grains. The result is a crudely hexagonal pseudo-cellular structure (Fig. 3).

A study of the thin sections of the wood shows that there are no resin canals and no apparent annual rings present (Fig. 1). The uniserial medullary rays are as many as twenty cells deep. There are one or two rows of bordered pits on the radial walls of the tracheids, contiguous, alternate and often slightly flattened. This identifies the wood generically as *Araucarioxylon*, a primitive coniferous type comparable to that found in the Arizona Triassic sandstones.

NATURE OF WOOD DURING SILICIFICATION

The condition of wood at the time of its petrifaction and the nature of the petrifying solutions have long been subjects of discussion. St. John[4] believes that wood may be either fairly fresh at the time of petrifaction, or it may be partly decayed.

---

[3] Stromer, E., Kraut, H. und Storz, M., Ergebnisse der Forschungsreisen Prof. E. Stromers in den Wusten Ägyptens. IV. Die fossilen Floren Ägyptens: *Abh. der Bay. Ak. der Wiss., Math.-natur. Abth.*, Neue Folge, **16**, 28, 42 (1933).

[4] St. John, Ruth N., Replacement vs. impregnation in petrified wood: *Econ. Geol.*, **22**, 730 (1927).

Wieland[5] suggests that much wood is probably partly lignitized before petrifaction, but he will not agree that vegetable matter has gone beyond the lightly carbonized stage to that of coaly matter, as suggested by earlier authors. He cites as evidence the lack of notable silicified bands in bituminous or anthracite coals.

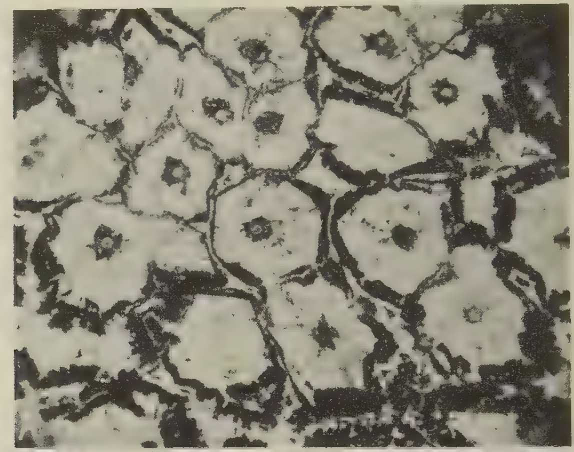

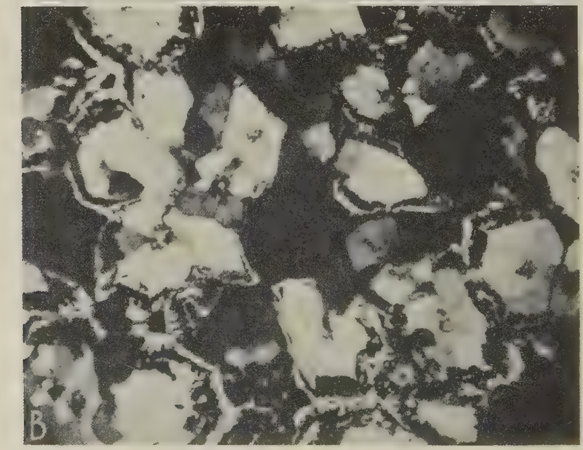

FIG. 3*a*. Transverse section of petrified wood illustrating hexagonal pseudo-cellular structure formed by the unusual cleansing action of the crystallizing quartz. Note the unharmed wood cells in the centers of the large clear areas. ×31.

FIG. 3*b*. Crossed nicols. Central dark area showing basal section of quartz hexagon. Note composite nature of some of the less perfectly formed hexagons. ×27.

---

[5] Wieland, G. R., Wood opalization: *Sci.*, *N.S.*, **76**, 278 (1932).

There is probably every gradation in condition of wood, just as there is every gradation from encrustation and penetration to complete replacement. Where there has been perfect preservation of the wood structure and form, as in the Nevada fine grained silcified woods, the structure must have been intact. In this investigation it has been found that the outer portions of the logs or stems are the ones preserved by coarse grained quartz with the development of the pseudocellular structure. The inner wood was evidently sound and the siliceous solutions preserved it. The outer wood had probably reached the lightly carbonized stage,* and its weakened cells were disrupted by the growing quartz crystals as they attempted to clear themselves.

Nature of Petrifying Solutions

The nature of siliceous petrifying solutions is a problem not yet solved. The majority of chemists and geologists believe that silica occurs and is transported only in the colloidal state in natural solutions.[6] Lovering,[7] investigating the solubility of silica and silicate minerals, found that cold water solutions of the bicarbonates of calcium and magnesium attacked all silica and silicate minerals, and to about the same degree. He accepted the belief that silica goes into solution as a colloid.

On the other hand Wieland[8] believes that monosilicic acid, thermal in source, must account for certain petrified forests.

Willstatter[9] has recently stated that conditions arise in nature where true silicic acid solutions result from acid action on silicates, and that the commonest solvent is carbonic acid. He presents H. Kraut's method for the production of orthosilicic acid in the laboratory, and discusses the factors that favor stability of the simplest silicic acid, namely its extreme dilution, or a slightly increased pressure to give a stronger carbonic acid and higher hydrogen ion concentration. If Willstatter and Kraut are correct in their assumptions that monosilicic acid can exist, the solutions which penetrated the dolomite beds to silicify the Triassic woods may have been true solutions. Certainly they must have been weak in silica and high in carbonate content. Willstatter makes a general assumption that colloidal silica lacks the ability to penetrate wood and animal membranes. Therefore, because silica does penetrate it must be in the form of a true molecular solution. This is not a safe assumption.

---

* That the black color of the wood is due to its carbonaceous content was demonstrated by firing several slices, 2–3 mm. thick, in a ceramics furnace at 1500° C. Upon cooling, the slice resembled white bath tile. Under the microscope, faint outlines of the wood structure, apparently due to the residual ash, can be seen.

[6] Weiser, G. B., *The Hydrous Oxides*, McGraw-Hill, N. Y., 178 (1926).

[7] Lovering, T. S., The leaching of iron protores, solution and precipitation of silica in cold water: *Econ. Geol.*, **18**, 523, 525 (1923).

[8] *Loc. cit.*, 279.

[9] Willstatter, Richard, Über Kieselsaurewanderung und Verkieselung in der Natur: *Natur und Museum Sencken. Naturf. Gesell.*, B. **61**, 332–337 (1931).

Bailey[10] has shown that the perforations in the pit membranes of conifers are of such size that aqueous solutions containing finely divided carbon can be made to pass through the membranes of the bordered pits of the sap wood of conifers. He also cites an experiment in which gelatin was passed through the septa of the bordered pits.[11] Bailey[12] also points out that experiments show re-soaked dry woods, in many cases, to be somewhat more pervious to air and presumably to solutions, than unseasoned material. This is probably due to the rupturing of the pit membranes during the process of drying.

SUMMARY AND CONCLUSIONS

1. The black petrified wood found in Upper Triassic dolomite beds of the Sonoma Range, Nevada, is preserved by the infiltration of siliceous material which crystallized as quartz.
2. Where the wood was sound, the quartz growth was influenced by the cell walls; where there was a weakened cell structure the crystallizing quartz, usually considered far down the crystalloblastic scale, was able to partially, if not completely, clear itself of the carbonaceous material and destroy the true cell structure.
3. The assumption, in proof of the existence to true molecular silicic acid, that coniferous woods act as dialyzers and, therefore, exclude colloidal solutions, is unwarranted in view of the work done by wood technologists and botanists on size of openings in cell walls.

---

[10] Bailey, Irving W., The structure of the bordered pits of conifers and its bearing upon the tension hypothesis of the ascent of sap in plants: *Bot. Gazette*, **62**, 133–142 (1916).

[11] *Ibid.*, 136.

[12] Bailey, Irving W., Preservative treatment of wood: *Forest Quarterly*, Mar. **1913.** Contrib. from the Lab. of Wood Tech. of Harvard School of For., No. **2**, p. 7.

MEASUREMENTS OF THE INDICES OF REFRACTION IN ANISOTROPIC MEDIA*

T. T. Quirke and W. C. Lacy

Contents

Abstract 705
Acknowledgments 705
Introduction 706
Measurement of ray directions 706
  Equipment and procedure 706
  Observations 711
    Circular half-cylinder 711
    Calculations of refraction of *e* ray 717
    Elliptical half-cylinder 718
    Bausch and Lomb optically true half-cylinder 721
Conclusions 724
References 724

ABSTRACT

Test pieces of calcite were prepared in order to measure directly the refraction of the ordinary and extraordinary rays in all crystallographic directions. Two half-cylinders were made from transparent calcite crystals; one being a semi-circle in cross section, and the other a half-ellipse. The dimensions of the ellipse were directly proportional to the values of the velocities of the extraordinary ray—parallel and normal to crystallographic *c* axis. The minor axis of the ellipse was made parallel to and the major axis normal to crystallographic *c*. The semi-circular specimen was cut with the crystallographic *c* parallel to the diameter. For both specimens observations were made on a goniometer with transmitted light. The ordinary ray emerged, refracted only at the surface of incidence of the semicircular cylinder, but the extraordinary wave normal was also refracted when leaving the calcite-air surface. The extraordinary ray was observed to follow a course in air after deflection at the surface of the calcite half-cylinder which agrees with the course to be expected according to computations. With the elliptical half-cylinder the extraordinary ray appeared to emerge from the calcite with almost no deflection from the computed course of the wave normal, and the ordinary ray, of course, was deflected.

In order to check the accuracy of the values obtained, observations were made on an optically true circular half-cylinder of identical size made by Bausch and Lomb Optical Company. This half-cylinder produced results essentially identical with those of the hand-made specimen.

The test pieces were difficult to make, but the results demonstrate clearly the behavior of the ordinary and extraordinary wave fronts in anisotropic media.

ACKNOWLEDGMENTS

The writers wish to express their appreciation to the Geological Society of America for its aid in this experimental work, to the National Youth Administration, for providing funds for drafting and computations, to Dr. G. M. Almy for his advice on certain optical phenomena, and to Dr. C. A. Chapman for many helpful suggestions.

---

* Part of Project No. 403, The Geological Society of America.

INTRODUCTION

The purpose of the series of experiments carried on by the authors was to analyze quantitatively the path of the ordinary and the extraordinary rays of light through an anisotropic substance for all angles of incidence and refraction, and to measure the index of refraction corresponding to each of these directions. This problem was suggested by the general confusion concerning this subject in textbooks of Mineralogy, Crystallography, and even in textbooks of Physical Optics, as noted by Tunell and Morey (1932), and more recently by Wooster (pp. 128 and 131).

Calcite, because of its high birefringence ($N_o - N_e = 0.1719$) and general use as an anisotropic illustrative mineral, was used in these experiments as the anisotropic medium.

MEASUREMENT OF RAY DIRECTIONS

Equipment and Procedure

Two half-cylinders were shaped from calcite crystals for the experimentation (Fig. 1). One half-cylinder, having a semi-circular cross-section with a 0.90 cm. radius and an altitude of approximately 1 cm., was cut so that prism face $(1\bar{1}00)$ lay parallel to the diameter of the semi-circle. The other half-cylinder having a semi-elliptical cross-section was cut so that the prism face $(1\bar{1}00)$ lay parallel to the minor axis of the ellipse. The ratio between the major and minor axes of the ellipse was directly proportional to the velocities of the extraordinary and ordinary rays, respectively (i.e., $2a = 20.00$ mm., $b = 11.155$ mm). The half-cylinder was approximately 1 cm. in height. These half-cylinders were formed by grinding down calcite crystals on steel molds.

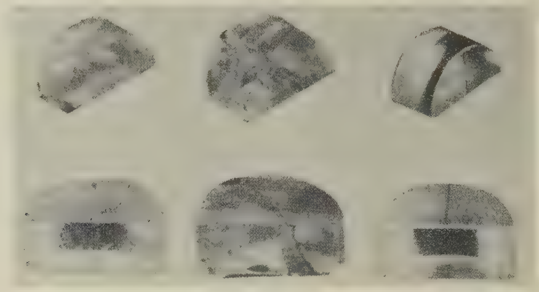

FIG. 1. Calcite test pieces cut in semi-circular and semi-elliptical forms with crystallographic c parallel to the diameter face. Two test pieces were hand-made and the third was made by the Bausch and Lomb Optical Company.

The semi-circular mold was formed by clamping together two blocks of steel, then drilling a hole of 1.8 cm. through them, using a point along the contact of the blocks as the center. By using two blocks the error which would result from the loss of thickness in sawing a single block in two was eliminated (Fig. 2). In the construction of the semi-elliptical mold an ellipse was drawn with its dimensions proportional to the elliptical ray surface originating from a point source of light in the anisotropic substance, calcite, as measured in a $(1\bar{1}00)$ section at the end of unit time (Fig. 2). This figure was drawn so that V_o/V_e or 0.67265/0.60304 = major axis/minor axis = 22.31mm./20.00 mm., and was divided along the minor axis—the direction of crystallographic *c*. From this drawing a special cutting tool was shaped which would cut a groove identical with the drawing. With this tool a groove of the specified proportions was cut in a steel block.

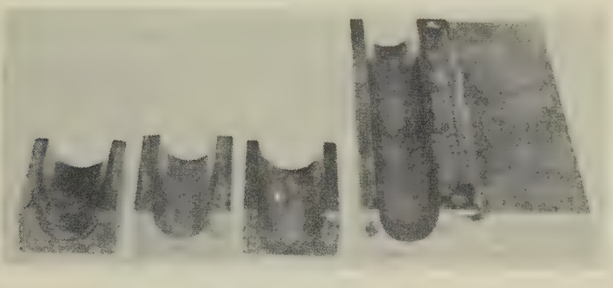

FIG. 2. Steel molds shaped for the grinding of the calcite test pieces.

A clear calcite crystal, free from flaws, was procured, and a section 1.8 cm. wide (measured along crystallographic *c*) and at least 1 cm. high, was cut from it. A prism face $(1\bar{1}00)$ was then selected for the flat face of the half-cylinder; it was smoothed down using a special abrasive[1] on a glass plate, and polished on a felt wheel using hematite rouge. This prism face was then cemented onto a glass microscope slide with De Khotinsky cement. The crystal segment was next ground down in the semicircular mold using 600 carborundum abrasive and keeping crystallographic *c* parallel to the diameter of the semi-circular cross-section. When the cylinder began to approximate the mold, the cylinder and the mold were thoroughly cleaned and the final grinding done with the finest abrasive. When the half-cylinder conformed exactly with the mold it was removed from the glass side and polished by hand, first on a felt wheel with hematite rouge, then on a buffer wheel. Great care was taken not to heat the cylinder in polishing, since it was found that heating caused splitting along the cleavage planes. It was also found that if alcohol or xylol were used in cleaning the cylinder a portion of the liquid soaked into the calcite, causing splitting along cleavage planes. The semi-elliptical half-cylinder was formed in a similar manner to that just described for the circular one, except that the crystal section cut at right angles to crystallographic *c* was exactly 20.00 mm. wide, and in grinding crystallographic *c* was kept parallel to the minor axis of the ellipse.

---

[1] Furnished by courtesy of the American Optical Company.

The orientation of the crystallographic directions in the half-cylinders was checked by the use of a polarizing microscope using the usual gypsum plate, sensitive tint, test. The half-cylinders were in turn placed on a glass slide, placed beneath the microscope and observed between crossed nicols. Observations were first made with the half-cylinder in an erect position lying on the $(\bar{1}2\bar{1}0)$ crystal plane. The extinction positions indicated the crystallographic directions, and any angle between the extinction position and the diameter of the semi-circular cross-section was noted. The half-cylinders proved to be correctly oriented with respect to crystallographic *c* with a possible error of ±30.′

The next step was to arrange a shield for the prism face of the half-cylinder to regulate the point of entrance of the light ray. First, the exact median line of the prism face was located, using a pair of dividers, and marked at the top and bottom of the half-cylinder. Next, two strips of tinfoil or thin copper sheeting, 1 cm.×1 cm., were cut and cemented to the face with rubber cement so that at the exact median line there was a gap between the shields of not more than 0.025 cm. With larger openings, the images transmitted through the calcite were very poorly defined, and with smaller openings the range of possible readings was greatly reduced.

The measurements of the angles of refraction of the light ray for varied angles of incidence upon the prism face $(1\bar{1}00)$ of the calcite half-cylinders were read directly on a Fuess one-circle goniometer #2a. This is the same instrument described in the Fuess catalog.

The first experiments were carried on only with the hand-made test pieces. The two half-cylinders of calcite were each subjected to similar experimental procedure. The cylinder was mounted on the stage and secured in position with plastic clay. The stage was then centered so that the cylinder revolved on an imaginary vertical line bisecting the prism face of the half-cylinder, and the narrow slit between the two copper shields, occupying the median line of the prism face coincided exactly with the vertical cross-hair of the telescope (Fig. 3). The stage was then rocked by means of the two cylindrical sections arranged at right angles to each other and having a common center, until the prism face of the half-cylinder was parallel to the vertical cross-hair, and the horizontal cross-hair struck the half-cylinder at the same height throughout a revolution of 360°. It was convenient to arrange the stage at such a height that the light image could be seen over the top of the cylinder. This was an aid in the rapid determination of the point of zero refraction. The stage was adjusted as to height by adjustment screw *k*.

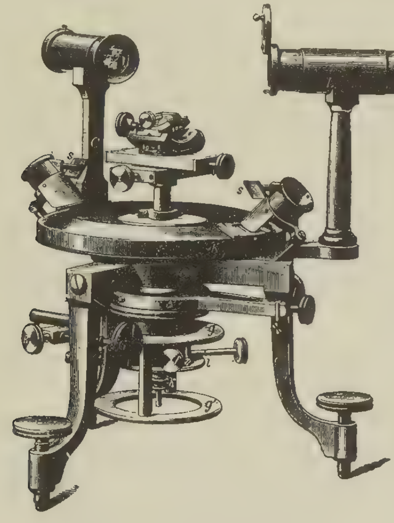

FIG. 3. A Fuess one-circle goniometer No. 2a. The various set-screws and parts are indicated by suitable letters for reference to the text.

A brilliant light source was placed behind the collimator tube *C*. In these experiments a white light source modified by a Websky slot placed in the rear of the collimator tube was used. The telescope, *L*, was focused on the light image by dropping the accessory lens from the system. The telescope was then swung around, lined up with the light image, and anchored by means of the gross motion screw α. The vernier was then turned until it read 0°, and anchored, using gross motion screw β. Fine adjustments were made with the tangential screw *G*.

The next step was to swing the stage, independent of the vernier, until the light from the collimator struck the prism face of the calcite half-cylinder with zero angle of incidence. This was accomplished by two methods. First, it was accomplished by the refraction method. The stage was slowly turned until the two images formed by the ordinary and extraordinary rays exactly coincided and fell on the vertical cross-hair of the aligned telescope.[2] At this point the angle of incidence of the light impinging upon the prism face was zero. Set-screw *l* was then tightened, thus locking the stage to the vernier. The second method used was a reflection method, in which the exact orientation of the prism face was determined by a beam reflected from its surface. Set-screw *l* was loosened, so that the stage swung freely independent of the vernier. The gross motion screw β was loosened, and the vernier turned so that it read 45° when the telescope was lined up with the light source and again anchored in this position. Fine adjustments were made with the tangential screw *G*. Gross motion screw α was then loosened and the telescope swung around until the vernier read 135°, and then anchored. The stage was then revolved until the light source was swung into view and lined up with the vertical cross-hair. The stage was then anchored to the vernier scale by means of set-screw *l*; the telescope was lined up with the light source and anchored; finally, the vernier and stage were turned until the vernier reading was 0°. At this point the angle of incidence of the light impinging upon the prism face of the half-cylinder was zero degrees. In these experiments both methods were used, one to check the other.

Following these preliminary adjustments the instrument was ready for making refraction readings on the calcite half-cylinder. Gross motion screw β was loosened and the stage swung around to the desired angle of incidence, anchored, and fine adjustments made with the tangent screw *G*. The angle of incidence was read directly from the vernier (Fig. 4). Gross motion screw α was then loosened and the telescope swung so that the two images of the ordinary and extraordinary rays were brought into view (Fig. 3). The identity of each of these rays was determined by means of a cap nicol placed over the eyepiece of the telescope. The vibration direction of the ordinary ray was vertical—perpendicular to crystallographic *c* and the vibration of the extraordinary ray was horizontal—in the plane of crystallographic *c*. The vertical cross-hair of the telescope was then centered on each of the light images—in cases of spectral dispersion the telescope was centered upon the yellow line—and the angle read directly from the vernier in each case (Fig. 4). The telescope was again lined up with the light source, anchored, and the stage revolved in the other direction in order to obtain an angle of incidence equal to that of the first but in the other quadrant of the half-cylinder.

---

[2] Some difficulty was encountered in this measurement in the circular half-cylinder due to a slight mal-alignment of the instrument. The image formed by the extraordinary image superimposed upon the ordinary image fell 37′ to the right of the vertical cross-hair. This error was corrected in the calculations by averaging the readings in the two quadrants of the half-cylinder.

The procedure was the same as in the first readings except that all of the readings were subtracted from 360° to obtain the angles of incidence and the angles of refraction. In these experiments readings were taken in this manner at intervals of 2° incidence from 0° to 60° for the circular half-cylinder. A few readings were obtained between 60° and 80°, but the images were not distinct. Due to structural defects in the circular cylinder, it was not possible to get a complete set of readings for both quadrants. However, for all angles of incidence between 0° and 60° refraction readings were obtained in one or both quadrants. Readings for the elliptical half-cylinder were taken at intervals of 5° incidence from 0° to 80°. A complete set of readings was obtained in both quadrants for this range.

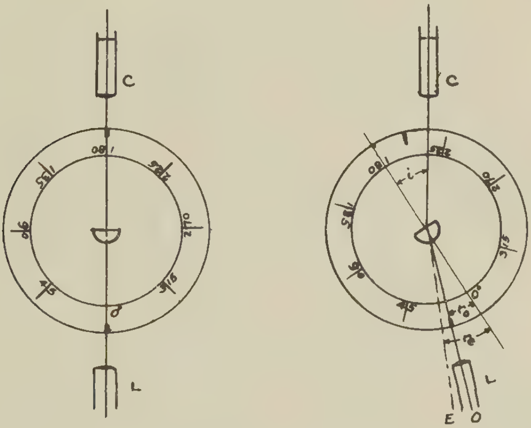

FIG. 4. Orientation of the instrument and test piece requisite for measurements of the angles of incidence and the refraction of the ordinary and extraordinary images.

OBSERVATIONS

Circular half-cylinder.—The angular measurements from opposite quadrants obtained from the refracted rays emerging from the calcite circular half-cylinder were averaged together, thus correcting for a slight mal-alignment of the goniometer. In cases where only one reading was available, the net reading was corrected for the 0°37′ instrumental malalignment.

The results obtained from the averaged angular measurements of the *o* ray correspond generally to the theoretical relation such that $\sin i/\sin r = 1.6583$ but with definite discrepancies. These discrepancies serve the very useful purpose of providing checks both as to the degree of accuracy

READINGS FROM CIRCULAR HALF-CYLINDER OF CALCITE
REFRACTION OF THE ORDINARY RAY

i	Right	Left	Average	Calculated	Difference between observation and theory
0°	−0°37′	+0°37′	0°00′	0°00′	
2°	—	—	—	—	
4°	—	—	—	—	
6°	—	5°00′	4°23′	—	
8°	—	6°18′	5°41′	—	
10°	6°35′	7°51′	7°13′	6°01′	+1°12′
12°	—	8°32′	—	—	
14°	8°35′	—	—	—	
16°	9°40′	—	—	—	
18°	10°44′	—	—	—	
20°	12°04′	12°24′	12°09′	11°54′	+0°15′
22°	—	13°30′	—	—	
24°	—	14°37′	—	—	
26°	—	15°46′	—	—	
28°	—	16°58′	—	—	
30°	17°18′	17°51′	17°35′	17°33′	+0°02′
32°	—	18°58′	18°33′	—	
34°	19°09′	19°44′	19°26′	—	
36°	19°57′	20°59′	20°28′	—	
38°	21°05′	22°00′	21°32′	—	
40°	22°04′	22°47′	22°36′	22°49′	−0°23′
42°	22°57′	23°36′	23°16′	—	
44°	23°43′	24°29′	24°03′	—	
46°	24°31′	25°26′	24°58′	—	
48°	25°44′	26°12′	25°58′	—	
50°	26°22′	27°05′	26°43′	27°31′	−0°48′
52°	27°18′	27°56′	27°37′	—	
54°	28°02′	28°47′	28°25′	—	
56°	29°00′	29°30′	29°15′	—	
58°	29°31′	30°12′	29°52′	—	
60°	30°19′	30°55′	30°37′	31°29′	−0°51′
70°	—	31°30′	31°10′	34°31′	−3°21′
75°	—	32°48′	32°28′	35°38′	−3°10′
80°	—	34°00′	33°40′	36°56′	−3°16′

REFRACTION OF THE EXTRAORDINARY RAY[3]
($I+r_{e_1}$)

i	Right	Left	Average	Calculated	Difference between observation and theory
0°	−0°37′	+0°37′	0°00′	0°00′	
2°	—	—	—	—	
4°	—	—	—	—	
6°	—	5°55′	—	—	
8°	—	7°29′	—	—	
10°	8°11′	8°57′	8°34′	7°20′	+1°14′
12°	—	10°15′	—	—	
14°	10°00′	—	—	—	
16°	11°18′	—	—	—	
18°	12°40′	—	—	—	
20°	14°13′	15°08′	14°40′	14°29′	+0°11′
22°	—	16°30′	—	—	
24°	—	17°55′	—	—	
26°	—	19°14′	—	—	
28°	—	20°27′	—	—	
30°	20°04′	21°49′	20°56′	21°15′	+0°41′
32°	—	23°04′	—	—	
34°	23°07′	24°20′	—	—	
36°	24°10′	25°22′	—	—	
38°	25°21′	26°31′	—	—	
40°	26°33′	27°33′	27°03′	27°27′	−0°24′
42°	27°33′	28°45′	—	—	
44°	28°34′	29°44′	—	—	
46°	29°30′	30°41′	—	—	
48°	30°40′	31°42′	—	—	
50°	31°34′	32°33′	32°04′	32°50′	−0°46′
52°	32°33′	33°32′	—	—	
54°	33°22′	34°07′	—	—	
56°	34°20′	34°58′	—	—	
58°	35°04′	35°56′	—	—	
60°	35°49′	36°38′	36°13′	37°24′	−1°11′
70°	38°35′	37°40′	38°08′	40°39′	−2°31′
75°	—	39°15′	—	—	
80°	—	40°00′	—	42°43′	−2°43′

---

[3] See Figure 7.

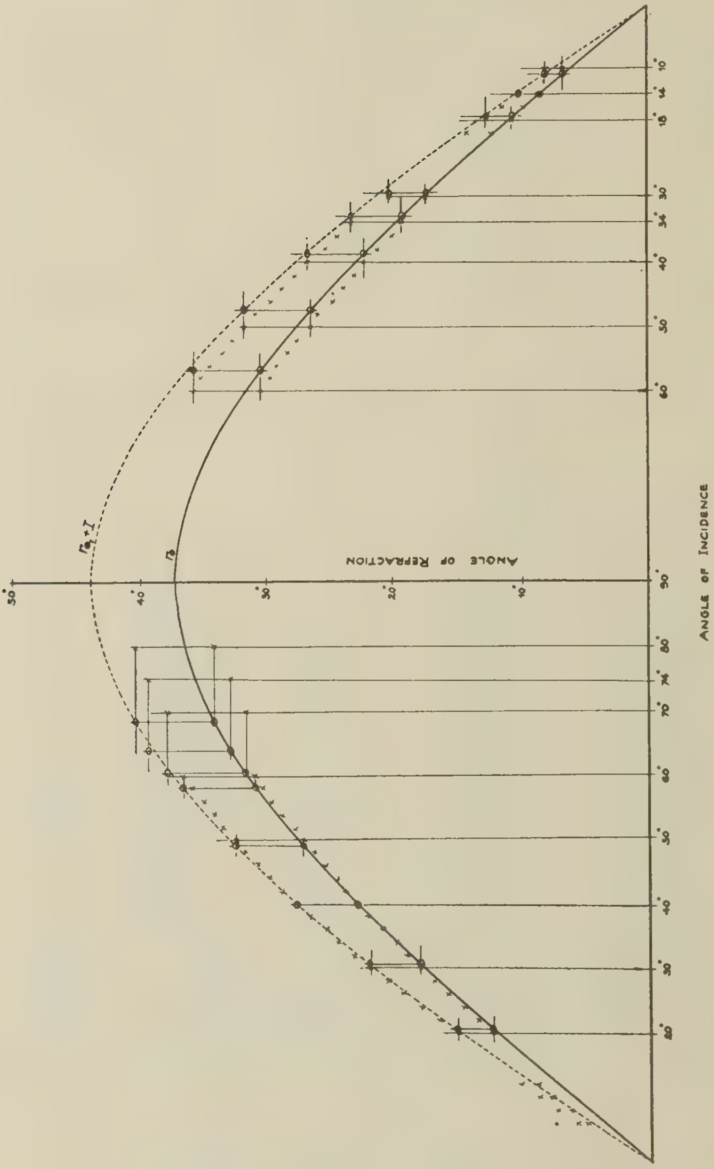

FIG. 5. Graph showing observational data and theoretical curves for the values of the ordinary and extraordinary rays transmitted through a calcite half-cylinder, in which crystallographic *c* lies in the diameter face of the half-cylinder. Errors due to irregularity of the test-piece have been corrected graphically. The circles indicate the points thus corrected. The solid curve is for the ordinary ray; the dashed curve is for the extraordinary ray, and crosses indicate actual readings.

of the observational data, and as as to how the handmade test pieces depart from true proportions, shaping, and optical orientation.

The angular measurements of the refracted *e* ray emerging from the calcite half-cylinder did not conform to values that might be expected at first thought from Huygen's wave construction. In accordance with Huygen's construction it would be expected that the *e* ray would have a smaller angle of refraction than that of the *o* ray (Fig. 6). However, in the direct measurements it was found that the measured angle of refraction for the *e* ray was considerably greater than that of either the *o* ray or of the wave normal of the *e* wave front, as calculated from theoretical values. The reasons for this discrepancy were made apparent in subsequent observations.

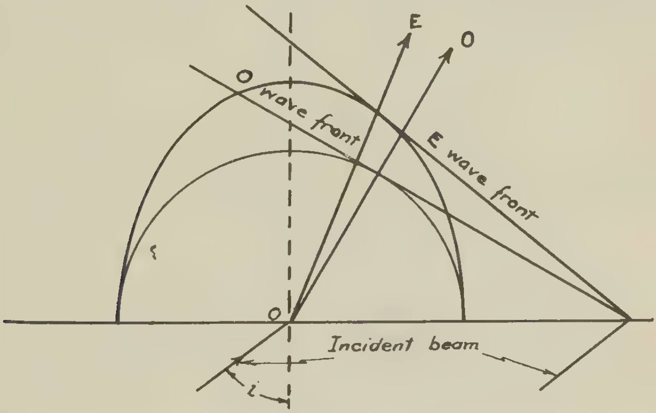

FIG. 6. Huygen's construction showing the paths of ordinary and extraordinary rays in an anisotropic medium and the resulting wave fronts.

In measuring the refraction of transmitted light through the circular half-cylinder the authors noted an unexpected behavior of the *o* and *e* rays. It was first noted that if the vertical cross-hair of the telescope was centered upon the distant light image with the *o* vibration direction and the focus changed to the surface of the cylinder, by throwing the accessory lens into the system, the vertical cross-hairs remained centered on the image. However, when the telescope was focused and centered upon the distant *e* image and the accessory lens thrown into the system, it was found that the image was thrown out of line with the vertical cross-hair of the telescope. Although the field was reversed due to the action of the accessory lens, the *e* image did not reverse its position in the field but remained on the same side of the *o* image in the observed field. Moreover, when an attempt was made to center the telescope on this image, the image would move a short distance in front of the vertical cross-hair, and then extinguish before the telescopic cross-hair could be centered upon it.

These observations indicated that the *o* ray came directly through the circular half-cylinder and left normal to the surface. The *e* ray, however, was refracted at the surface of the half-cylinder and crossed the path of the *o* ray. This conclusion was demonstrated simply by the use of a small shield of copper sheeting. This shield was inserted across the field of view between the half-cylinder and telescope at different distances from the rear surface of the half-cylinder, and the order of disappearance of the images noted (Fig. 7). At position *a*, the copper shield being in contact with the rear surface of the half-cylinder, the *o* image was the first to disappear. When the shield was inserted in position *b*, a few mm. from the rear surface of the half-cylinder the two images disappeared simultaneously, and in position *c*, 10 cm. from the surface of the half-cylinder, the *e* image was the first to extinguish.

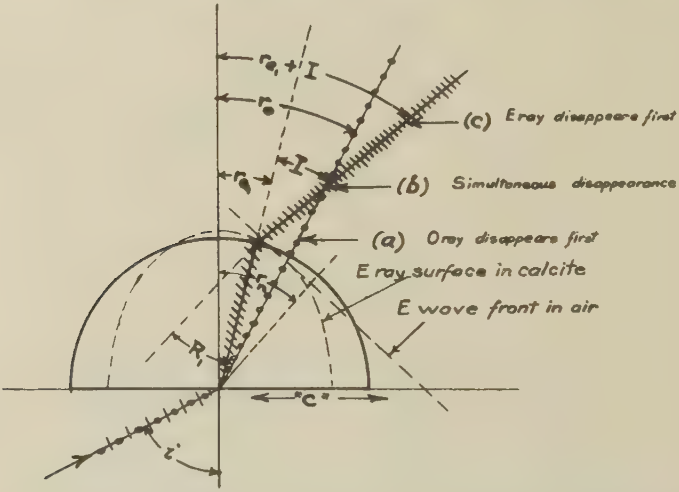

FIG. 7. Diagram to indicate the refraction of the extraordinary wave normal as it left the circular half-cylinder of calcite.

This phenomenon was examined also by projecting the two light images onto a translucent paper screen which was then moved outward from the calcite surface. At the surface of the calcite two distinct images were observed on the screen. As the screen was moved outward these images were observed to converge, and at about 3 mm. distance from the surface the images coalesced. Beyond this point of coincidence the images separated and continued to diverge with increased distance from the calcite surface.

These demonstrations proved conclusively that the *o* ray had traveled through the anisotropic medium, struck the calcite-air contact normal to the surface and emerged without refraction at that surface. The wave front of the ordinary ray is parallel to the tangent of the circular surface of the calcite. The *e* ray, however, traveled through the anisotropic medium, struck the calcite-air contact normal to the surface but was refracted at the surface. The explanation of this refraction depends upon the vibration of the electro-magnetic disturbances of the *e* ray being oblique to the ray, although parallel to the tangent of the elliptical *e* ray surface, which is the extraordinary wave front. Consequently, the vibration directions of the *e* ray, being parallel to the extraordinary wave front were oblique to the ordinary wave front, and as a result suffered refraction at the calcite-air surface of the half-cylinder. This refraction can be calculated, and thereby the observed values may be checked.

Calculations of refraction of e ray.—Malus discovered the relationship $O/E \tan r_0 = \tan r_{e_1}$, where O and E are the standard velocities of the ordinary and extraordinary rays respectively, $\tan r_0$ is the angle of refraction of the *o* ray, and $\tan r_{e_1}$, the angle of refraction of the *e* ray (Fig. 7). It can also be shown that $E/O \tan r_0 = \tan r_n$, where r_n is the angle of refraction of the extraordinary wave normal. Then $r_n - r_e =$ the angle of refraction, R_1, of the extraordinary wave normal at the calcite-air surface at the point of emergence of the extraordinary ray. The index of refraction at this point can be determined from the relationship $\mu_{\epsilon_1} = \sin i / \sin r_n$, where i is the angle of incidence of the light upon the prism face of the half-cylinder. I, the direction taken by the E ray disturbance as it emerges from the calcite into air, can be calculated from Snell's Law: $\sin I = \sin R_1 \mu_{\epsilon_1}$. The computations are summarized below.

The similarity between the observed and calculated values will be noted (Fig. 5). Examination of the data show small but consistent departures from agreement between observation and theory. With the aid of the data provided by observations of the ordinary ray, one may see that there is a definite lack of true shape in the test-piece. Furthermore, it may be noted that the direction and amount of discrepancy disclosed by the ordinary ray observations nearly coincide with the apparent errors in the data derived from the extraordinary ray observations. By a simple change in the recorded angle of incidence to correspond to the actual angle of refraction, based on the ordinary ray data, one may shift also the position of the extraordinary ray readings to correspond to the same angle of incidence. This has been done for the points recorded, with the result that the observed data of the extraordinary ray became amazingly close to their theoretical values. This correction, which seems quite

TABLE OF COMPUTATIONS

i	r_0*	r_{e_1}	r_n	$r_n - r_{e_1} (= R_1)$	μ_{ϵ_1}	I	$r_{e_1} + I$*
10°	6°01′	5°24′	6°42′	1°19′	1.4801	1°57′	7°20′
15°	8°59′	8°04′	10°00′	1°56′	1.4903	2°53′	10°57′
20°	11°54′	10°42′	13°14′	2°32′	1.4941	3°47′	13°14′
25°	14°46′	13°18′	16°23′	3°05′	1.4997	4°37′	17°55′
30°	17°33′	15°50′	19°26′	3°36′	1.5028	5°25′	21°15′
35°	20°14′	18°17′	22°21′	4°04′	1.5084	6°09′	24°26′
40°	22°49′	20°40′	25°09′	4°29′	1.5125	6°47′	27°27′
45°	25°15′	22°55′	27°45′	4°50′	1.5185	7°21′	30°16′
50°	27°31′	25°07′	30°10′	5°03′	1.5243	7°43′	32°50′
55°	29°36′	26°59′	32°22′	5°23′	1.5301	8°15′	35°14′
60°	31°29′	28°52′	34°20′	5°28′	1.5355	8°31′	37°24′
65°	33°08′	30°20′	36°04′	5°44′	1.5396	8°51′	39°11′
70°	34°31′	31°45′	37°30′	5°45′	1.5446	8°54′	40°39′
75°	35°38′	32°43′	38°39′	5°56′	1.5465	9°12′	41°55′
80°	36°26′	33°36′	39°28′	5°52′	1.5494	9°07′	42°43′
85°	36°56′	33°58′	39°59′	6°01′	1.5504	9°21′	43°19′

* The data for r_0 and for $r_{e_1} + I$ were used to construct the theoretical curves in Figures 5, 8 and 10.

logical and legitimate, appears to bear out completely the analysis of the phenomena here advanced, and to confirm the accuracy of the computations involved.

Elliptical half-cylinder.—Measurements of the refraction angles for varied angles of incidence in the calcite elliptical half-cylinder were recorded only for the extraordinary ray. The ordinary ray of course suffered added refraction at the calcite-air surface but was disregarded as not being pertinent to this study.

READINGS FROM ELLIPTICAL HALF-CYLINDER OF CALCITE
REFRACTION OF WAVE NORMAL[4]

i	Erect (1)		Inverted (2)	
	Right	Left	Right	Left
10°	7°43′	6°44′	7°08′	7°19′
15°	11°03′	10°01′	10°31′	10°39′
20°	14°05′	13°06′	13°35′	13°40′
25°	17°01′	15°59′	16°26′	16°40′
30°	20°08′	19°01′	19°28′	19°42′
35°	23°11′	21°53′	23°18′	23°35′
40°	25°41′	24°30′	25°04′	25°15′
45°	28°20′	26°40′	27°44′	27°53′
50°	30°12′	29°02′	30°07′	—
55°	32°13′	30°58′	32°11′	—
60°	33°45′	33°03′	33°55′	—
65°	35°08′	34°25′	35°11′	—
70°	35°57′	—	36°00′	—
80°	36°41′	—	—	—

COMPARISON OF OBSERVATION WITH THEORETICAL VALUES

i	Calculated values of r_n	Average readings (Position 1)	Difference between observation and Theory	Average readings (Position 2)	Difference between observation and theory
10°	6°42′	7°14′	+0°31′	7°13′	+0°32′
20°	13°14′	13°36′	+0°21′	13°38′	+0°24′
30°	19°26′	19°34′	+0°08′	19°35′	+0°09′
40°	25°09′	25°06′	−0°03′	25°09′	−0°00′
50°	30°10′	29°37′	−0°43′	30°07′	−0°03′
60°	34°20′	33°24′	−0°56′	33°55′	−0°25′
70°	37°30′	35°51′	−1°39′	36°00′	−1°30′
80°	39°28′	36°41′	−2°47′	—	—

---

[4] Readings were taken only on the refracted images of the *e* ray; these represent the angle of refraction of the wave normal at the point of emergence. Four sets of readings were obtained, one in each quadrant for the erect half-cylinder, and one in each quadrant of the same half-cylinder in an inverted position.

Inasmuch as the extraordinary ray emerged with very little or no refraction, it follows that the wave normals must have emerged normal to the calcite-air surface (Fig. 9). The extraordinary ray of course traveled through the elliptical half-cylinder in a path similar to that taken in the circular half-cylinder for the same angle of incidence. However, the *e* ray emerged from the elliptical half-cylinder normal to the calcite-air surface and also normal to the extraordinary wave front. Consequently, the angular readings obtained from the extraordinary ray at the point of emergence from the elliptical half-cylinder gave directly the refraction of the extraordinary wave normal, r_n. The results obtained from the measurements of the *e* ray corresponded very closely with the respective theoretical values as calculated for the normal to the *e* wave front at the point of emergence of the *e* ray (Fig. 8). This similarity proves that the half-cylinder very closely approximated the shape of the extrordinary ray surface.

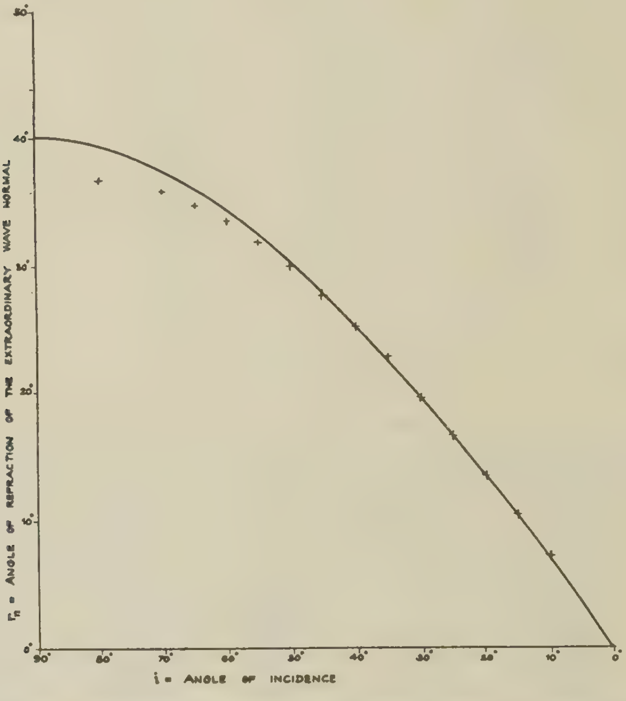

FIG. 8. Graph showing the actual readings plotted against the curve, representing observed and theoretical values for the refraction of the wave normal in calcite. These readings were made from an elliptical half-cylinder, so proportioned that the axes of the ellipse are the same relatively as the velocity of the ordinary and extraordinary rays.

The differences between observation and computed values are to be ascribed mainly to the fact that the ellipse was not quite true in shape, being 35/1000th (35 mils) of an inch too long in the major axis for the theoretically correct dimensions. The measurements were actually 770 mils in diameter and 463 ± 4 mils high. The true proportions require 428 mils for the height. The specimen was measured with a micrometer screw. Furthermore, optical measurements with a petrographic microscope showed that the diameter face, supposedly parallel to the crystallographic *c*, was actually inclined $2° \pm \frac{1}{2}°$ to the correct direction. During an attempt to regrind this test-piece to correct the imperfections, unfortunately it was cracked too seriously to afford further readings. In spite of its physical shortcomings, the elliptical test-piece seems to have served to demonstrate that the ray surface in calcite is an ellipse, and that the wave normal leaves the ellipse normal to the tangent at the point of emergence.

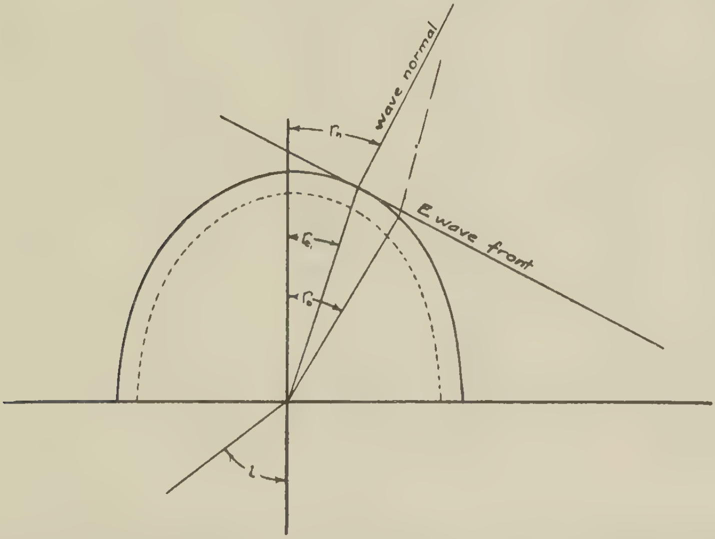

FIG. 9. Diagram following Huygen's construction to show that from an elliptical test-piece, whose curvature equals that of the ray surface ellipse, the extraordinary wave normal will emerge without refraction at the calcite-air surface.

Bausch and Lomb optically true half-cylinder.—In order to check the accuracy of the results obtained from the hand-made circular half-cylinder and to estimate the relative accuracy which could be expected from the elliptical half-cylinder with dimensions similar to those of the hand-made specimen (Fig. 1) Bausch and Lomb prepared an optically true half-cylinder. It was found that the average readings from the hand-made cylinder were consistently higher than the refraction readings on the Bausch and Lomb piece.

BAUSCH AND LOMB CIRCULAR HALF-CYLINDER OF CALCITE[5]
ANGLE OF REFRACTION OF THE ORDINARY RAY

i	Right	Left	Average	Calculated	Difference between observation and Theory
10°	6°03′	6°00′	6°01′	6°01′	0°00′
15°	8°57′	8°52′	8°55′	8°59′	−0°04′
20°	11°56′	11°50′	11°53′	11°54′	−0°01′
25°	14°43′	14°37′	14°40′	14°46′	−0°06′
30°	17°30′	17°24′	17°27′	17°32′	−0°05′
35°	20°10′	20°04′	20°07′	20°14′	−0°07′
40°	22°36′	22°30′	22°33′	22°49′	−0°16′
45°	25°02′	24°55′	24°59′	25°15′	−0°16′
50°	27°16′	27°19′	27°17′	27°31′	−0°14′
55°	29°06′	29°20′	29°13′	29°36′	−0°23′
60°	30°55′	31°15′	31°05′	31°29′	−0°24′
65°	32°26′	32°51′	32°38′	33°08′	−0°30′
70°	33°39′	34°08′	33°24′	34°31′	−0°07′
75°	34°27′	35°06′	34°46′	35°38′	−0°52′
80°	34°56′	35°30′	35°13′	36°26′	−1°13′
85°	34°37′	35°24′	35°00′	36°56′	−1°56′
89°30′	—	35°21′	—	—	—

ANGLE OF REFRACTION OF THE EXTRAORDINARY RAY[6]
$(r_{e_1}+I)$

i	Right	Left	Average	Calculated	Difference between observation and Theory
10°	7°23′	7°20′	7°21′	7°20′	+0°01′
15°	11°03′	10°57′	11°00′	—	
20°	14°33′	14°27′	14°30′	14°29′	+0°01′
25°	18°00′	17°54′	17°57′	—	
30°	21°16′	21°10′	21°13′	21°15′	−0°02′
35°	24°27′	24°21′	24°24′	—	
40°	27°25′	27°20′	27°23′	27°27′	−0°04′
45°	30°07′	30°02′	30°05′	—	
50°	32°41′	32°45′	32°43′	32°50′	−0°07′
55°	34°55′	35°07′	35°01′	—	
60°	36°57′	37°15′	37°06′	37°24′	−0°18′
65°	38°36′	39°04′	38°50′	—	
70°	40°00′	40°30′	40°15′	40°39′	−0°24′
75°	40°53′	41°31′	41°12′	—	
80°	41°28′	42°13′	41°50′	42°43′	−0°53′
85°	41°13′	42°00′	41°36′	—	
89°30′	—	41°58′	—	—	

---

[5] Readings were made with sodium light.

[6] See Figure 7.

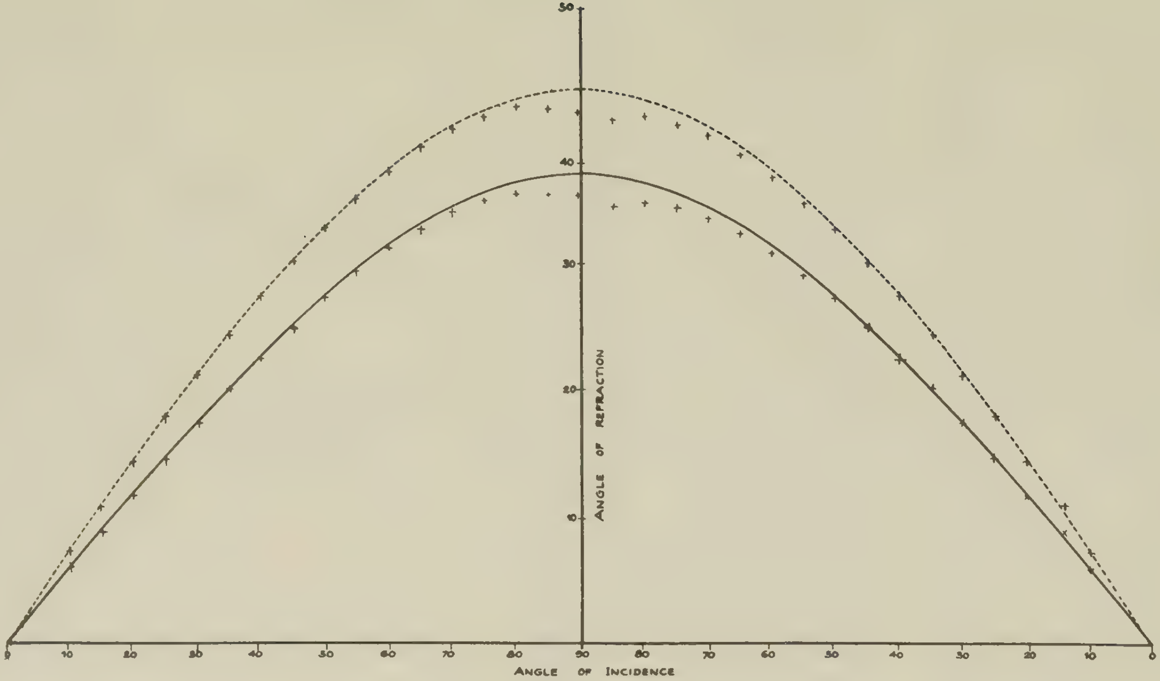

FIG. 10. Graph showing data and theoretical values from the ordinary and extraordinary rays when transmitted through a nearly optically true calcite half-cylinder. The test-piece was provided by the Bausch and Lomb Optical Company. This may be compared with Fig. 5. Note that much fewer corrections are required to reconcile observations with theory.

There seems to be a definite tendency for the observed data to fall lower than their theoretical value as the angles of incidence get higher. This shows clearly with all test-pieces. However, using the simple corrections applied to the first cylinder also to this second piece, close agreement results. A similar degree of error should be expected in the elliptical half-cylinder observations. There were no corrections made in this instance, but the smoothness of the curves derived by plotting the data, and the close correspondence of these readings to the theoretical values, indicate that the experiments thoroughly confirm the theoretical analysis.

CONCLUSIONS

These experiments furnish a simple and conclusive demonstration of the relation between the directions of the ordinary and extraordinary rays and wave normals and the corresponding indices of refraction in anisotropic media. However, the actual making of the test-pieces, provided one has suitable calcite crystals, is a procedure requiring considerable care and patience.

REFERENCES

TUNELL, GEORGE, AND MOREY, GEORGE W., Some correct and some incorrect statements of elementary crystallographic theory and methods in current text-books: *Am. Mineral.*, **17**, 365–380 (1932).

WOOSTER, W. A., *A Text-book on Crystal Physics*. Cambridge (1938).

NOTES AND NEWS

SERENDIBITE AND ASSOCIATED MINERALS FROM THE NEW CITY QUARRY, RIVERSIDE, CALIFORNIA

GERALD M. RICHMOND, *Harvard University, Cambridge, Mass.*

OCCURRENCE

The limestone bodies near Riverside, California, have long been famous as mineral localities. At the New City Quarry, two miles south of Riverside, the marble has been invaded by the Bonsall tonalite. Serendibite, a complex calcium, aluminum, magnesium silicate has been recently found among the contact minerals by Professor E. S. Larsen. The mineral has been previously described from Gangapitija, Ceylon, by Coomáráswámy (1) and from Warren County, New York, by Larsen and Schaller (2).

The rock is a grey, coarse grained dolomitic marble. Predazzite, a calcite-brucite mixture, has formed in bands parallel to the bedding as a result of the dissociation of the dolomite. As is common in hydrothermal contact metamorphic rocks, the replacement products are variable. In part they are parallel to the bedding, in part they are less regular. Although the collection made at the quarry represents only a few hours observations, the following minerals, which may be divided into four groups on their general paragenetic relation, were observed in the laboratory.

Thermal	*Early hydrothermal*	*Middle hydrothermal*	*Late hydrothermal*
graphite	allanite	biotite	brucite
magnetite	apatite	hornblende	chlorite
periclase	diopside	microcline	clinozoisite
	grossularite	orthoclase	hydromagnesite
	hedenbergite	plagioclase	limonite
	idocrase	quartz	magnetite
	serendibite	scapolite ($Ma_{49}Me_{51}$)	nontronite
	spinel (pleonaste?)	tremolite	phlogopite
	wollastonite		sericite

SERENDIBITE

Serendibite occurs as a massive granular aggregate in thin irregular replacement bands in the limestone which it replaces incompletely. No crystal forms have been observed. In the hand specimen the color is dark blue with a glossy lustre. It is intimately associated with diopside as an early hydrothermal-contact-metamorphic replacement mineral of the limestone. Plagioclase feldspar, of a late hydrothermal stage, is likewise found associated with serendibite. It varies in composition from andesine to labradorite and replaces the limestone and diopside.

The serendibite is optically positive, and has an axial angle of nearly 90°. The indices of refraction and pleochroism are as follows.

Riverside	New York
$\alpha=1.719$, pale yellow green.	$\alpha=1.701$, very pale yellow green.
$\beta=1.722$, pale blue green.	$\beta=1.703$, nearly colorless.
$\gamma=1.724$, brilliant sky blue.	$\gamma=1.706$, prussian blue.

It is interesting to note that the indices are markedly higher than those of the material reported by Larsen and Schaller from New York. This is probably due to a higher percentage of iron. However, there was not enough of the material available for an analysis. The mineral has an extremely strong dispersion, $r>v$, which causes unusual interference colors and indistinct extinction. It likewise has a low birefringence. Broad polysynthetic twins are common.

NONTRONITE

A common rock from the quarry is a coarse aggregate of labradorite feldspar and hedenbergite. The pyroxene is in large part altered to nontronite, a greenish yellow earthy mineral having a fibrous or micaceous structure. It is biaxial negative, and has a small axial angle. The indices vary considerably but are about: $\alpha=1.566$, $\beta=1.583$, $\gamma=1.586$. Extinction is generally indistinct because of the fibrous nature of the mineral.

REFERENCES

(1) COOMÁRÁSWÁMY, A. K., The crystalline limestones of Ceylon: *Quart. Jour. Geol. Soc., London,* **58,** 420–422 (1902).

(2) LARSEN, E. S., AND SCHALLER, W. T., Serendibite from Warren County, New York, and its paragenesis: *Am. Mineral.,* **17,** 457–465 (1932).

NEW ACCESSIBILITY OF THOMSONITE BEACH, MINNESOTA

FRANKLIN B. HANLEY,
University of Minnesota, Minneapolis, Minn.

With the completion of the relocating and hard surfacing of the Minnesota portion of the Lake Superior International Highway (U. S. #61), the Thomsonite Beach zeolite locality on the north shore of Lake Superior in Cook County, Minnesota, is now quickly and easily accessible. It is from this area that the finest and most highly prized specimens of semiprecious thomsonite and allied zeolites have been obtained. In addition to thomsonite, N. H. Winchell[1] identified mesolite, lintonite, and scolecite.

---

[1] Winchell, N. H., *Minn. Geol. & Nat. Hist. Surv,* Final Report, **5,** 248–251; 405–409 (1900).

The collecting ground is approximately 105 miles northeast of Duluth and 5½ miles southwest of Grand Marais, in Sec. 34, T. 61 N., R. 1 W. This is the "Grand Marais" locality cited in mineralogical literature. Thomsonite Beach lies almost exactly 4 miles "beyond" (northeast) the Cascade River, lakeward from where the new highway makes a sweeping curve just before entering a 40 foot cut. A convenient parking turnout is located at the west end of the long guard fence at the beginning of the curve. Several indistinct trails lead to the lake which is only about 300 feet from the road.

The easily accessible portion of the shore at this point is about ¼ mile long. It is low, rock-bound, and relatively straight and consists of the upper portion of a thick amygdaloidal basalt flow of Keweenawan age. The flow dips at a low angle (10°–15°) to the south passing beneath the surface of the lake. At this line of contact a low wave-cut cliff is generally present.

Thomsonite Beach, in a restricted use of the term, is a small pocket beach about 65 feet across, located some 100 yards from Terrace Point, the eastern termination of this segment of the shore. Good Harbor Bay lies beyond to the north and east. Unfortunately, for the past several years the surface of this small beach has been covered with basalt cobbles and other coarse debris.

The primary occurrence of the zeolites is as amygdules, commonly from ¼ to ½ inch in diameter, and as fillings along joint planes in the flow. As a secondary occurrence, when released from the enclosing basalt, they tend to accumulate through wave action as water-worn pebbles in the pocket beaches and small rock basins along the shore. The new highway cut mentioned above penetrates what appears to be the same flow that is exposed at the edge of the water. Fresh material may be obtained from the walls and from blocks of this basalt dumped along the sides of the adjacent fills.

Erratum

The American Mineralogist, **24,** 478 (1939), in the article on "brochantite," line 5 from bottom should read "$X \wedge a$ nearly 13°. $X = 1.728$."

NEW MINERAL NAMES

Priceite

W. F. FOSHAG: Priceite from Furnace Creek, Inyo County, California. *Am. Mineral.*, **9**, 11–13 (1924).

CHEMICAL PROPERTIES: A hydrous borate of calcium, $5CaO \cdot 6B_2O_3 \cdot 9H_2O$. CaO 32.5, B_2O_3 48.7, H_2O 18.8. Insoluble in water, soluble in acids.

CRYSTALLOGRAPHICAL PROPERTIES: Triclinic?, minute rhombic plates with 58° angle.

PHYSICAL AND OPTICAL PROPERTIES: Color white, luster earthy to porcelainous. Fracture conchoidal, brittle. Hd. 3–3.5. G. 2.43. Compact cryptocrystalline. Biaxial, negative. $2V=32°$. $\alpha=1.572$, $\beta=1.591$, $\gamma=1.594$.

Priceite from Oregon and pandermite from Turkey have been shown to be identical.[1] Although "pandermite" was frequently mentioned by the miners as present in borax beds, this mineral has proven, upon examination, to be howlite. True priceite was found only at one locality, at Furnace Creek Wash, Inyo County, California. The first specimens found occurred as nodules and irregular masses, embedded in a soft greenish gray shale associated with colemanite and gypsum (selenite). Later it was found as veins or narrow lenses in shale a foot or more thick and up to 10 feet long. This priceite is compact and broken into numerous angular fragments, due apparently to shrinkage in its change from a colloidal to a metacolloidal form. Other priceite was found as filling cracks in a dark olive green altered basalt hillock near the mouth of Corkscrew Canyon. At both of the latter occurrences the priceite was altered in part to delicate radiating needles of ulexite, or to sharp crystals of colemanite. Still another occurrence of priceite is as amydule fillings in the altered basalts, some of them reaching the size of a large potato.

W. F. FOSHAG

DISCREDITED SPECIES

Molengraaffite

C. E. TILLEY: The identity of molengraaffite with lamprophyllite. *Trans. Geol. Soc. S. Africa*, **41**, 109–111 (1938).

A new partial analysis of molengraaffite from Pilansberg gave: CaO 1.9, SrO 14.4, BaO 1.8. The original analysis, therefore, appears to be in error, SrO and BaO being included in the CaO. This identity is confirmed by a comparison of optical properties.

W. F. F.

---

[1] Larsen, Esper S., *Am. Mineral.*, **2**, 1–3 (1917).